3D analytical prediction of building damage due to ground subsidence produced by tunneling

Authors: Carles Camós[1]* and Climent Molins[1]

Affiliations:

[1]Universitat Politècnica de Catalunya. Jordi Girona 1-3, C1-206, 08034 Barcelona (Spain)

*Corresponding author: carles.camos-andreu@upc.edu

Abstract: Tunnel construction entails the generation of ground settlements, which can endanger the adjacent buildings. The prediction of damages in buildings is usually based on the classical Gaussian profiles for the approximation of the subsidence trough and the equivalent beam method for modeling the response of building walls. Current available expressions refer to walls aligned transversally with respect to the tunnel axis, which usually represents the worst-case scenario. However, approximations must be done for other building alignments, since no analytical expressions are available for these cases. We propose a novel equation for the determination of the horizontal ground strain, which departs from the equations of the classical Gaussian settlement profiles. The novel formulation allows the application of the equivalent beam method in 3D and the modeling of the tunnel advance. The results show significant variations of the estimated damage depending on the wall position with respect to the tunnel axis. The paper reviews also certain relevant aspects of building damage predictions, such as the influence area of settlements and the possible contribution of ground horizontal strain to damage reduction. A parametric analysis is further performed to create a non-linear regression model that allows direct estimation of the maximum tensile strain in a building wall according to input values of geological conditions and wall and tunnel geometries.

Keywords: Tunnel construction, settlements, building damage, analytical prediction.

1. Introduction

1.1 *Background*

Design of urban tunnels requires the prediction of possible damages in adjacent buildings produced by tunneling subsidence. The use of Finite Element Models is appropriate for the estimation of damages, including the location and width of crack patterns (Giardina et al. 2013). However, primary assessments of the response of buildings to settlements can be done with the equivalent beam method (Burland & Wroth, 1974; Boscardin & Cording, 1989), which is widely used in tunneling engineering. This method models a building wall as a weightless linear elastic beam subjected to a given ground settlement profile. Strains in the beam are generated (a) due to the deflection when conforming to the settlement profile and (b) due to the ground horizontal strain generated on the base of the beam. The distribution of strains along the beam depends on the mode of deformation, which comprises a combination of bending and shear. For this reason, two extreme modes are typically considered in order to ascertain which is the most critical: pure

bending and pure shear. Maximum tensile strains in the beam due to pure bending (ε_{br}) and pure shear (ε_{dr}) deformations are given by the following expressions derived from the elastic beam theory:

$$\varepsilon_{br} = (\varepsilon_{bmax} + \varepsilon_h) \tag{1}$$

$$\varepsilon_{dr} = \varepsilon_h \left(1 - \frac{E}{4G}\right) + \sqrt{\frac{\varepsilon_h^2}{16}\left(\frac{E}{G}\right)^2 + \varepsilon_{dmax}^2} \tag{2}$$

where E/G is the ratio between the Young and shear moduli of the wall material, ε_{bmax} and ε_{dmax} are the maximum strains due to the deflection of the beam in pure bending and pure shear modes of deformation (Sec. 4) and ε_h is the value of horizontal ground strain on the base of the beam, which depends on the shape of the settlement trough and on the location of the wall (Figure 1). This location is defined by the proximity and the alignment with respect to the tunnel axis (Sec. 2). The maximum tensile strain ε_{max} corresponds to the highest value between ε_{br} and ε_{dr} along the beam. Based on ε_{max}, the approach of Burland et al. (1977) is used in this paper for classification of the damage magnitudes (Sec. 4).

The determination of ε_{max} represents a 3D problem that depends on (a) the ground conditions, (b) the building geometry, (c) the tunnel geometry, (d) the building position with respect to the tunnel axis, (e) the location of the tunnel face and (f) the construction technology. Nevertheless, equivalent beam analyses are usually simplified and performed in 2D. For example, in case of buildings aligned transverse to the tunnel axis (x-direction), data evidence has shown that the shape of the settlement profile S can be closely approximated to a Gaussian probability density distribution (Peck, 1969). The settlement profile in the longitudinal direction (y-direction) is usually described by a Gaussian cumulative distribution function (Attewell & Woodman, 1982). Settlement profiles in both directions are depicted in Figure 1.

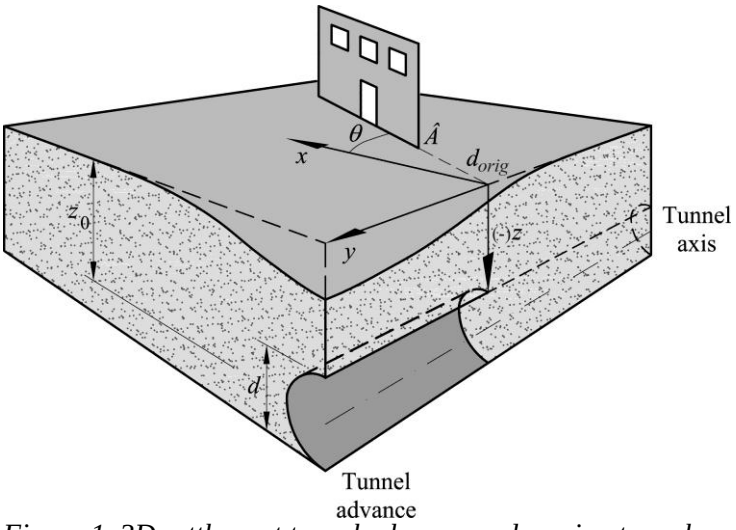

Figure 1. 3D settlement trough above an advancing tunnel.

Expressions of ground horizontal movements in the transverse $U_x(x)$ and longitudinal $U_y(y)$ directions with respect to the tunnel axis were given by O'Reilly & New (1982) by assuming that ground particles move towards the tunnel axis. Horizontal ground strain ε_h in the transverse

$\varepsilon_{h,xx}(x)$ and longitudinal $\varepsilon_{h,yy}(y)$ directions are directly given by derivation of $U_x(x)$ and $U_y(y)$:

$$\varepsilon_{h,xx}(x) = \frac{dU_x(x)}{dx} \tag{3}$$

$$\varepsilon_{h,yy}(y) = \frac{dU_y(y)}{dy} \tag{4}$$

Buildings walls aligned transversally and longitudinally with respect to the tunnel axis are statistically representative, since many urban tunnels follow the tracks of avenues or streets. However, there are a significant number of buildings randomly aligned with respect to tunnel axes, in particular when using a Tunnel Boring Machine (TBM). The damage assessment in these cases is usually simplified by projecting the transverse or the longitudinal (whichever is the closest) settlement profile along the axis of the rotated wall, as shown in Figure 2 (Kappen J., 2012; Camós, Molins et al. 2014). However, this practice can become unrealistic for alignments far from the transverse or longitudinal cases. Therefore, the determination of ε_h and the posterior damage assessments using this practice may be inaccurate.

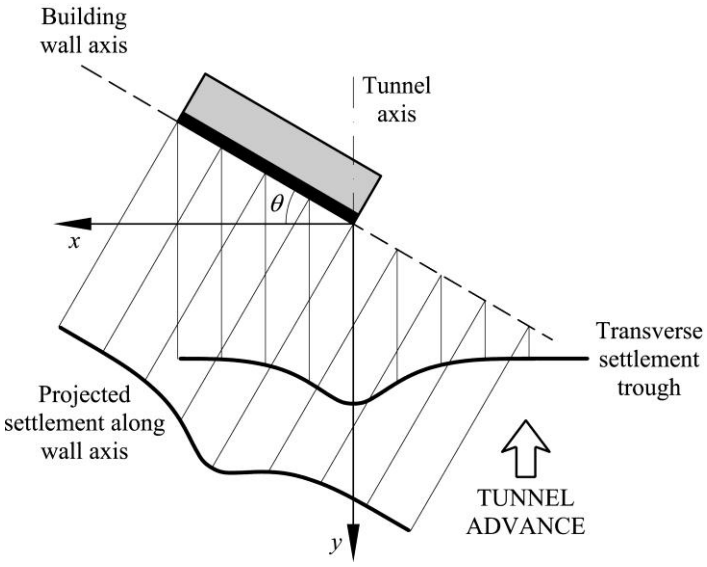

Figure 2. Projection of settlement profile in case of a rotated building respect to x-direction.

The models of Peck (1969), Attewell & Woodman (1982) and O'Reilly & New (1982) can be extended to obtain 3D expressions for the settlement trough, $S(x,y,z)$, the ground horizontal displacements, $U_x(x,y,z)$ and $U_y(x,y,z)$ and the ground horizontal strains, $\varepsilon_{h,xx}(x,y,z)$ and $\varepsilon_{h,yy}(x,y,z)$ (see Sec. 2). However, no equation has been found in the literature to determine the resultant value of ε_h in a particular wall alignment. Therefore, accurate estimations of ε_h can only be achieved with the use of numerical simulation and hence, the complete analytical assessment of building damage cannot be performed. Moreover, numerical simulation is commonly avoided in practice due to the required computation resources and modeling expertise (Giardina et al. 2012).

1.2 *Objective and approach*

The present paper proposes a novel equation for the exact determination of ε_h in a particular wall alignment by applying a change of basis to the infinitesimal ground strain tensor (Sec. 2). The new equation departs from the equations of Peck (1969), Attewell & Woodman (1982) and O'Reilly & New (1982), which assume that settlement troughs produced by tunneling construction are Gaussian-shaped. The proposed equation is used to show the influence of the ground conditions and the tunnel geometry in the values of ε_h (Sec. 3). The paper furthermore reviews certain relevant aspects of building damage predictions with the equivalent beam method in 3D, such as the influence area of settlements and the possible contribution of ground strain to damage reduction. The influence of the tunnel face location and the position of the building wall in the damage assessment is also shown by means of a parametric analysis (Sec. 4). The resulting data is used to create a non-linear regression model that allows the direct estimation of the maximum tensile strain ε_{max} in a building wall according to input parameters of the geological conditions and the wall and tunnel geometries (Sec. 5).

2. **Development of a novel equation for the ground horizontal strain $\boldsymbol{\varepsilon_h}$ in 3D**

2.1 *Description of the building wall position*

The next sections describe the development of a novel equation for the determination of the resultant ground strain ε_h in a particular wall alignment θ with respect to the tunnel axis. For this reason, the notation for the description of the building wall position is given, first for a general case (Sec. 2.1.1) and then for the particular case of building walls parallel to tunnel axis (Sec. 2.1.2).

2.1.1 *General case*

A typical tunneling situation with a building wall of length l_{build} is depicted in Figure 3. The y-axis follows the tunnel longitudinal axis, whereas the x-axis corresponds to a transverse plane to the tunnel. The origin of the coordinates will be set at the intersection between the wall and the tunnel longitudinal axes. Note that this coordinate system refers to a particular wall and must be changed when other walls are analyzed.

The tunnel face is located at coordinate y_s and advances towards $y = -\infty$, following the criteria set by Attewell et al. (1986). y_f represents the location of the tunnel portal.

The wall is aligned θ degrees with respect to the tunnel transverse plane. Counterclockwise alignments are considered positive ($\theta > 0$). The distance between the wall reference point $\hat{A}$ and the origin of coordinates is named d_{orig}. For convenience, this distance can also take negative values. Wall positions can be described with this notation within a range of $\theta = [-90°, 90°]$ and $d_{orig} = (-\infty, +\infty)$. However, note that due to symmetry of the settlement trough about the tunnel longitudinal axis, wall positions described by $d_{orig} = d_{orig_1}$, such that $0 > d_{orig_1} \geq -l_{build}$ with $\theta = \theta_1 \epsilon [-90°, 90°]$ are equivalent with the position described by $\theta_2 = -\theta_1$ and $d_{orig_2} = \left|d_{orig_1}\right| - l_{build}$ (see cases d) and e) in Figure 4).

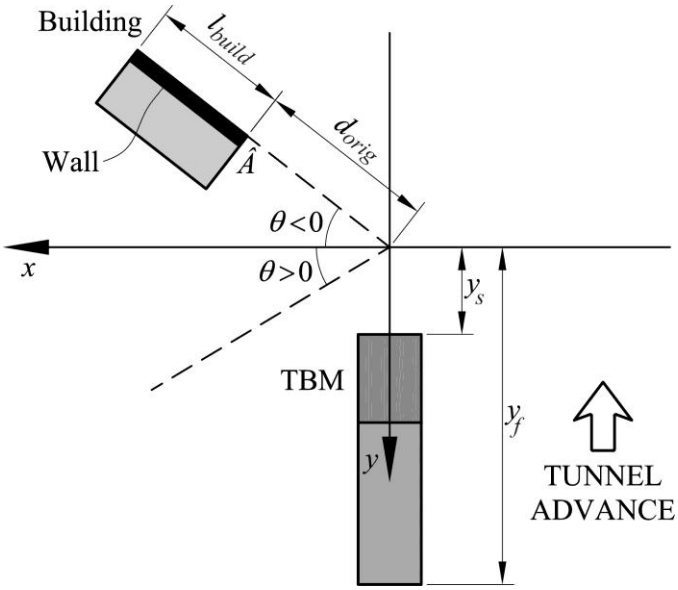

Figure 3. Parameters of tunnel and building positions (general case)

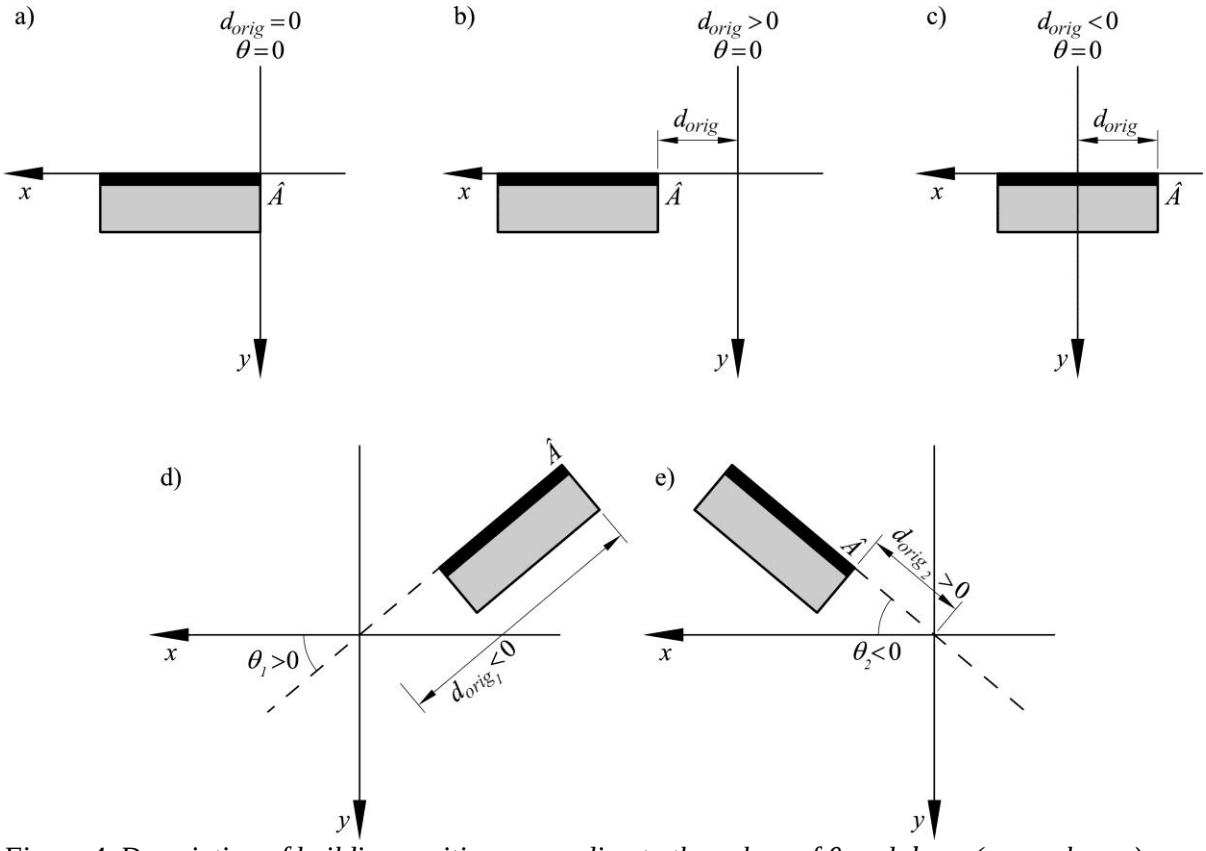

Figure 4. Description of building positions according to the values of θ and d_{orig} (general case)

2.1.2 *Building wall parallel to tunnel axis*

All wall positions can be described with the notation of Sec. 2.1.1 except the cases of building walls parallel to the tunnel longitudinal axis. In this case, the x-axis is set at the same coordinate y of the wall reference point $\hat{A}$ (Figure 5). The wall is located at a distance d_{axis} from the tunnel

axis. This distance is defined in a range $(-\infty, +\infty)$. Due to symmetry, the cases with $d_{axis} < 0$ have the equivalent case on the positive side. Case of $d_{axis} = 0$ can be treated with both notations (the one shown in Sec. 2.1.1 and the present one).

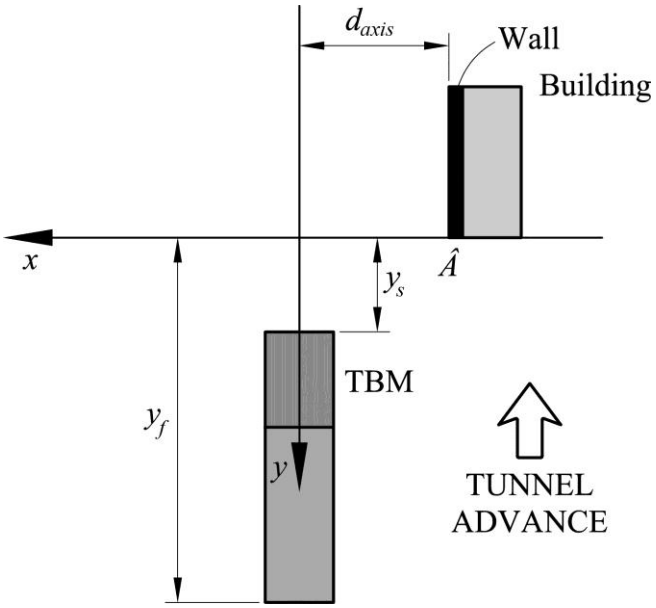

Figure 5. Parameters of tunnel and building position (case of parallel walls with respect to the tunnel axis).

2.2 *Description of 3D settlement Gaussian trough*

The settlement in [mm] at a certain position with coordinates x, y, z in [m] is calculated by the expression (Peck, 1969; Attewell & Woodman, 1982; O'Reilly & New, 1982):

$$S = -1000 \cdot S_{max} \cdot exp\left[-\frac{x^2}{2 \cdot K_x^2 \cdot (z_0 - z)^2}\right] \cdot \cdot \left[\Phi\left(\frac{y - (y_s + y_0)}{K_y \cdot (z_0 - z)}\right) - \Phi\left(\frac{y - y_f}{K_y \cdot (z_0 - z)}\right)\right] \quad (5)$$

where S_{max} is the absolute value of maximum settlement far behind the tunnel face, where the deformations are fully developed. It is calculated as:

$$S_{max} = \frac{V_L \cdot \pi \cdot d^2}{\sqrt{2\pi} \cdot K_x \cdot (z_0 - z) \cdot 4} \quad (6)$$

d and z_0 are the tunnel diameter and depth of the tunnel axis in [m], respectively, with z_0 being a positive magnitude. $\Phi(.)$ is the standard normal cumulative distribution function. Note that term of $\Phi(.)$ that contains y_f becomes 0 if $y_f = +\infty$. V_L is the volume ground loss per unit, K_x and K_y are the non-dimensional shape parameters describing the Gaussian settlement curves in the transverse and longitudinal direction respectively. K_x and K_y depend on the type of soil: high values of the parameter indicate flat/broad settlement curves (stiff or soft silty clays), whereas low values indicate sharp/narrow settlement curves (granular soils). The products $K_x \cdot z_0$ and $K_y \cdot z_0$ determine the location of the inflection points $i_x = i_y = i$ of the Gaussian curves. Note

that settlements S in Eq. (5) are considered to be negative along the z-axis. It is important to keep this sign convention for the correct application of related equations of ground horizontal displacements and strain (see Secs. 2.3-2.4). However, references to settlement magnitudes will be expressed in absolute values throughout the paper.

It is commonly assumed that the settlement above the tunnel face corresponds to half the maximum settlement S_{max}, which occurs at a distance far behind from the tunnel face. However, it has been shown that this value can be lower depending on the type of ground and the construction technology (Nomoto et al. 1995, Fargnoli et al. 2013). For example, the tunnel pressure of a TBM shield in soft soils restricts the ground movements on the heading, so that the major part of the settlements is related to the tail void. For this reason, a new parameter y_0 has been introduced in the original equation in order to model the shift of the longitudinal settlement profile with respect to the tunnel face position (Figure 6). This parameter can be deduced from the equation of Attewell & Woodman (1982) for the surface longitudinal settlement at the tunnel centerline ($x = z = 0$), with the tunnel portal location far from tunnel face ($y_f = +\infty$). This profile is described by a Gaussian cumulative distribution function:

$$|S(x = z = 0, y)| = S_{max} \cdot \Phi\left(\frac{y - y_0}{i_y}\right) \tag{7}$$

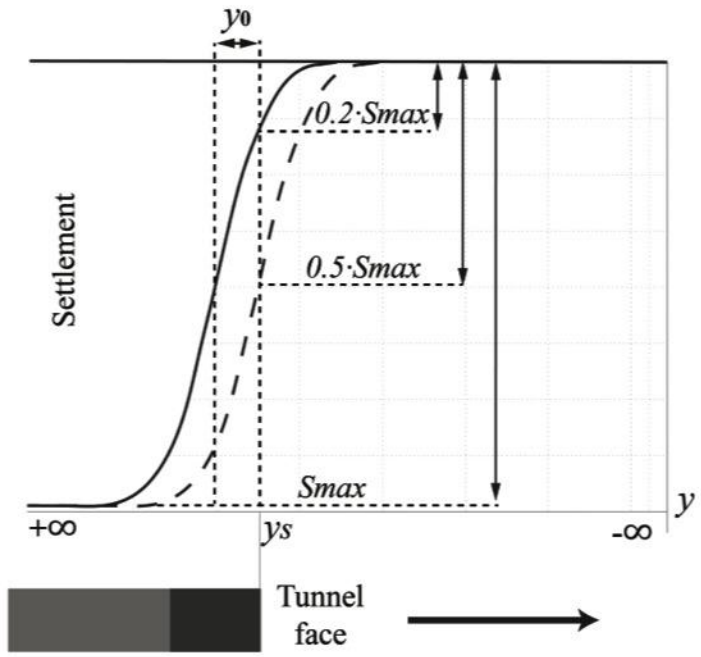

Figure 6. Longitudinal settlement profiles for δ =0.2 (solid line) and δ =0.5 (dashed line)

The settlement above the tunnel face ($y = y_s$) is:

$$|S(x = z = 0, y = y_s)| = S_{max} \cdot \Phi\left(\frac{y_s - y_0}{i_y}\right) \tag{8}$$

Rearranging Eq. (8) and setting $i_y = K_y \cdot z_0$, the expression of the shift of the longitudinal settlement results in:

$$y_0 = -\Phi^{-1}(\delta) \cdot K_y \cdot z_0 \tag{9}$$

where δ is the ratio between the surface settlement above the tunnel face and the maximal settlement S_{max} at infinite distance behind of the face:

$$\delta = \frac{|S(x = z = 0, y = y_s)|}{|S(x = z = 0, y = +\infty)|} = \frac{|S(x = z = 0, y = y_s)|}{S_{max}} \tag{10}$$

An example of shifted longitudinal settlement profile for a δ ratio equal to 0.2 is also shown in Figure 6.

2.3 *Ground horizontal displacements*

Horizontal displacements in [mm] in the transverse (U_x) and longitudinal (U_y) directions with respect to the tunnel axis at a certain position with coordinates x, y, z in [m] are given by (O'Reilly & New,1982):

$$U_x = \frac{x}{z_0 - z} \cdot S \tag{11}$$

$$U_y = 1000 \cdot \frac{V_L \cdot d^2}{8 \cdot (z_0 - z)} \cdot \left[exp\left(\frac{-\left(y - (y_s + y_0)\right)^2 - x^2}{2 \cdot K_y^2 \cdot (z_0 - z)^2} \right) - exp\left(\frac{-\left(y - \left(y_f\right)\right)^2 - x^2}{2 \cdot K_y^2 \cdot (z_0 - z)^2} \right) \right] \tag{12}$$

Where S is given by Eq. (5).

2.4 *Ground horizontal strains*

2.4.1 *Equations for the 3D field*

The fields of strains (per unit) in the transverse ($\varepsilon_{h,xx}$) and longitudinal ($\varepsilon_{h,yy}$) directions respect to the tunnel axis are directly given by derivation of the field of ground displacements:

$$\varepsilon_{h,xx} = \frac{\partial U_x}{\partial x} = \frac{\frac{S}{1000}}{z_0 - z} \cdot \left(1 - \left(\frac{x^2}{K_x^2 \cdot (z_0 - z)^2} \right) \right) \tag{13}$$

$$\varepsilon_{h,yy} = \frac{\partial U_y}{\partial y} = \frac{V_L \cdot d^2}{8 \cdot (z_0 - z)} \cdot \left[\left(\frac{-2y + 2(y_s + y_0)}{2 \cdot K_y^2 \cdot (z_0 - z)^2} \right) \cdot exp\left(\frac{-\left(y - (y_s + y_0)\right)^2 - x^2}{2 \cdot K_y^2 \cdot (z_0 - z)^2} \right) - \left(\frac{-2y + 2\left(y_f\right)}{2 \cdot K_y^2 \cdot (z_0 - z)^2} \right) \cdot exp\left(\frac{-\left(y - \left(y_f\right)\right)^2 - x^2}{2 \cdot K_y^2 \cdot (z_0 - z)^2} \right) \right] \tag{14}$$

The resultant of ε_h along an alignment θ in the range $(-90°, 0°) \cup (0°, 90°)$ is not directly given with Eqs. (13) and (14). For this reason, a basis transformation of the infinitesimal strain tensor

is used to find the resultant value $\hat{\varepsilon}_{h,\widehat{xx}}$ in a direction $\hat{x}$ that matches with the building wall alignment θ for which ε_h is being determined.

Let $\boldsymbol{\varepsilon}$ be the infinitesimal strain tensor described with the orthonormal basis $\{\boldsymbol{e_1}, \boldsymbol{e_2}, \boldsymbol{e_3}\}$, where $\boldsymbol{e}_1 = (1,0,0)$, $\boldsymbol{e}_2 = (0,1,0)$, $\boldsymbol{e}_3 = (0,0,1)$ represent the directions x, y, z of the reference Cartesian coordinate system (note that $S \equiv U_z$):

$$\boldsymbol{\varepsilon} = \begin{bmatrix} \varepsilon_{h,xx} & \varepsilon_{h,xy} & \varepsilon_{h,xz} \\ \varepsilon_{h,yx} & \varepsilon_{h,yy} & \varepsilon_{h,yz} \\ \varepsilon_{h,zx} & \varepsilon_{h,zy} & \varepsilon_{h,zz} \end{bmatrix} = \begin{bmatrix} \dfrac{\partial U_x}{\partial x} & \dfrac{1}{2}\left(\dfrac{\partial U_x}{\partial y} + \dfrac{\partial U_y}{\partial x}\right) & \dfrac{1}{2}\left(\dfrac{\partial U_x}{\partial z} + \dfrac{\partial S}{\partial x}\right) \\ \dfrac{1}{2}\left(\dfrac{\partial U_y}{\partial x} + \dfrac{\partial U_x}{\partial y}\right) & \dfrac{\partial U_y}{\partial y} & \dfrac{1}{2}\left(\dfrac{\partial U_y}{\partial z} + \dfrac{\partial S}{\partial y}\right) \\ \dfrac{1}{2}\left(\dfrac{\partial S}{\partial x} + \dfrac{\partial U_x}{\partial z}\right) & \dfrac{1}{2}\left(\dfrac{\partial S}{\partial y} + \dfrac{\partial U_y}{\partial z}\right) & \dfrac{\partial S}{\partial z} \end{bmatrix} \tag{15}$$

According to the tensor transformation theory, the infinitesimal strain tensor described in a new orthonormal basis $\hat{\boldsymbol{e}}_1, \hat{\boldsymbol{e}}_2, \hat{\boldsymbol{e}}_3$ is given by:

$$\hat{\boldsymbol{\varepsilon}} = \boldsymbol{L}\boldsymbol{\varepsilon}\boldsymbol{L}^{\boldsymbol{T}} \tag{16}$$

And,

$$\hat{\boldsymbol{\varepsilon}} = \begin{bmatrix} \hat{\varepsilon}_{h,\widehat{xx}} & \hat{\varepsilon}_{h,\widehat{xy}} & \hat{\varepsilon}_{h,\widehat{xz}} \\ \hat{\varepsilon}_{h,\widehat{yx}} & \hat{\varepsilon}_{h,\widehat{yy}} & \hat{\varepsilon}_{h,\widehat{yz}} \\ \hat{\varepsilon}_{h,\widehat{zx}} & \hat{\varepsilon}_{h,\widehat{zy}} & \hat{\varepsilon}_{h,\widehat{zz}} \end{bmatrix} \tag{17}$$

Where the components of matrix $\boldsymbol{L}$ are defined as:

$$l_{ij} = \hat{e}_i \cdot e_j \tag{18}$$

If the vector $\hat{\boldsymbol{e}}_1$ matches the longitudinal direction $\hat{x}$ of a wall with alignment θ, the new orthonormal basis is then given by $\hat{\boldsymbol{e}}_1 = (\cos\theta, \sin\theta, 0)$, $\hat{\boldsymbol{e}}_2 = (-\sin\theta, \cos\theta, 0)$, $\hat{\boldsymbol{e}}_3 = \boldsymbol{e}_3 = (0,0,1)$. Then, the components of the tensor transformation matrix $\boldsymbol{L}$ result in: $l_{11} = \cos\theta$, $l_{12} = \sin\theta$, $l_{13} = 0$, $l_{21} = -\sin\theta$, $l_{22} = \cos\theta$, $l_{23} = 0$, $l_{31} = 0$, $l_{32} = 0$ and $l_{33} = 1$. Note that the change of basis represents a rotation of θ degrees counterclockwise about $\boldsymbol{e}_3$.

By multiplying matrices, the resultant horizontal strain along a particular wall alignment θ is given by:

$$\varepsilon_h \equiv \hat{\varepsilon}_{h,\widehat{xx}} = \cos^2\theta \cdot \varepsilon_{h,xx} + \sin^2\theta \cdot \varepsilon_{h,yy} + 2 \cdot \cos\theta \sin\theta \cdot \varepsilon_{h,xy} \tag{19}$$

Note that if the wall is perpendicular to the tunnel axis (i.e. $\theta = 0°$), Eq. (19) reduces to $\varepsilon_h = \varepsilon_{h,xx}$, whereas if the wall is aligned with the tunnel longitudinal axis (i.e. $\theta = \pm 90°$), Eq. (19) reduces to $\varepsilon_h = \varepsilon_{h,yy}$. By definition of the infinitesimal strain tensor, $\varepsilon_{h,xy}$ is given by:

$$\varepsilon_{h,xy} = \varepsilon_{h,yx} = \frac{1}{2}\left(\frac{\partial U_x}{\partial y} + \frac{\partial U_y}{\partial x}\right) \tag{20}$$

Terms $\frac{\partial U_x}{\partial y}$ and $\frac{\partial U_y}{\partial x}$ in Eq.(20) are given by derivation of Eqs. (11) and (12) (check Annex A for further details on the development of Eq. (21)):

$$\frac{\partial U_x}{\partial y} = \frac{x}{z_0 - z} \cdot (-S_{max}) \cdot \left(exp\left(-\frac{x^2}{2 \cdot K_x^2 \cdot (z_0 - z)^2} \right) \right) \cdot \left(\frac{1}{\sqrt{2\pi}} e^{-\frac{\left(\frac{y-(y_s+y_0)}{K_y \cdot (z_0 - z)}\right)^2}{2}} \cdot \left(\frac{1}{K_y \cdot (z_0 - z)} \right) - \frac{1}{\sqrt{2\pi}} e^{-\frac{\left(\frac{y-y_f}{K_y \cdot (z_0 - z)}\right)^2}{2}} \cdot \left(\frac{1}{K_y \cdot (z_0 - z)} \right) \right) \cdot \tag{21}$$

And,

$$\frac{\partial U_y}{\partial x} = \frac{V_L \cdot d^2}{8 \cdot (z_0 - z)} \cdot \frac{(-2x)}{2 \cdot K_y^2 \cdot (z_0 - z)^2} \left[exp\left(\frac{-\left(y - (y_s + y_0)\right)^2 - x^2}{2 \cdot K_y^2 \cdot (z_0 - z)^2} \right) - exp\left(\frac{-\left(y - (y_f)\right)^2 - x^2}{2 \cdot K_y^2 \cdot (z_0 - z)^2} \right) \right] \tag{22}$$

2.4.2 *Equations for building walls parallel to tunnel axis*

If the determination of settlements, ground horizontal displacements and strains is performed for the case of walls parallel to tunnel axis ($S_{par}, U_{y,par}$ and $\varepsilon_{h,par}$, respectively) the latter expressions are reduced to a 2D problem:

$$S_{par} = -1000 \cdot S_{max} \cdot exp\left[-\frac{{d_{axis}}^2}{2 \cdot K_x^2 \cdot (z_0 - z)^2} \right] \cdot \left[\Phi\left(\frac{y - (y_s + y_0)}{K_y \cdot (z_0 - z)} \right) - \Phi\left(\frac{y - y_f}{K_y \cdot (z_0 - z)} \right) \right] \tag{23}$$

$$U_{y,par} = 1000 \cdot \frac{V_L \cdot d^2}{8 \cdot (z_0 - z)} \cdot \left[exp\left(\frac{-\left(y - (y_s + y_0)\right)^2 - {d_{axis}}^2}{2 \cdot K_y^2 \cdot (z_0 - z)^2} \right) - exp\left(\frac{-\left(y - (y_f)\right)^2 - {d_{axis}}^2}{2 \cdot K_y^2 \cdot (z_0 - z)^2} \right) \right] \tag{24}$$

$$\varepsilon_{h,par} \equiv \hat{\varepsilon}_{h,\widehat{xx},par} = \frac{\partial U_{y,par}}{\partial y} = \tag{25}$$

$$\frac{V_L \cdot d^2}{8 \cdot (z_0 - z)} \cdot \left[\left(\frac{-2y + 2(y_s + y_0)}{2 \cdot K_y^2 \cdot (z_0 - z)^2} \right) \cdot exp\left(\frac{-\left(y - (y_s + y_0)\right)^2 - {d_{axis}}^2}{2 \cdot K_y^2 \cdot (z_0 - z)^2} \right) \right.$$
$$\left. - \left(\frac{-2y + 2\left(y_f\right)}{2 \cdot K_y^2 \cdot (z_0 - z)^2} \right) \cdot exp\left(\frac{-\left(y - \left(y_f\right)\right)^2 - {d_{axis}}^2}{2 \cdot K_y^2 \cdot (z_0 - z)^2} \right) \right]$$

where d_{axis} is the horizontal distance between tunnel and wall longitudinal axes shown in section 2.1.2. Note that $\hat{\varepsilon}_{h,\widehat{xx},par}$ corresponds to $\varepsilon_{h,yy}$ of Section 2.4.1.

2.4.3 *Definition of sagging and hogging deflection zones*

The nature of ground horizontal strains ε_h (compressive or tensile) has implications on the damage assessment. This nature is defined by the curvature or concavity of the settlement profile: zones with upwards concavity are known as sagging deflection zones, whereas downwards concavity refers to hogging deflection. The inflection points of the Gaussian settlement profiles delimit these zones. Sagging zones imply the generation of compressive strains ($\varepsilon_h < 0$) and hence, a favorable contribution to damage reduction. Hogging zones imply the generation of tensile strains ($\varepsilon_h > 0$), which will increase damages on the wall (Burland, 2008). In the remainder of the paper, compressive ground strains will be written as ε_{h-} and tensile, ε_{h+}.

3. **Variation of ground horizontal strain $\boldsymbol{\varepsilon_h}$ with the alignment $\boldsymbol{\theta}$**

3.1 *Introduction*

Next sections go deeper into the variation of the ground horizontal strain ε_h with the alignment θ, which may play a key role in the building damage assessment. The novel formulation shown in Sec. 2.4.1 is used for this purpose. For the ease of illustration, a particular example of the evolution of ε_h with θ during the tunnel face approximation is shown in Sec. 3.2. ε_h is further calculated for a wide range of ground conditions and tunnel geometries in a parametric analysis. The goal is to determine critical values of θ, regarding the value of ε_h (Sec. 3.3). Optimization techniques are used for this objective.

In the following we limit ourselves to the case of $K_x = K_y = K$, as it is often assumed in tunneling design (Attewell et al., 1986). The tunnel portal is considered at infinite distance from the face, i.e. $y_f = +\infty$.

3.2 *Representation of the field of ground horizontal strain ε_h*

Equations (13), (14) and (20)-(22) are referred to the Cartesian coordinate system with components x, y and z. However, cylindrical coordinates will be here used instead for making easier the visualization of the next plots. The following transformation is applied:

$$\begin{cases} x = r \cdot cos\,\theta \\ y = r \cdot sin\,\theta \\ z = z \end{cases} \quad (26)$$

where r is the horizontal distance between the z-axis and whichever ground point $\hat{P}$ located along the rotated $\hat{x}$-axis. The position of $\hat{P}$ can be described then by the coordinates $(r_{\hat{P}}, \theta_{\hat{P}}, z_{\hat{P}})$. However, the following analysis is only performed at ground surface, i.e. $z = 0$ and hence, coordinates of $\hat{P}$ can be given only by $(r_{\hat{P}}, \theta_{\hat{P}})$ (see Figure 7).

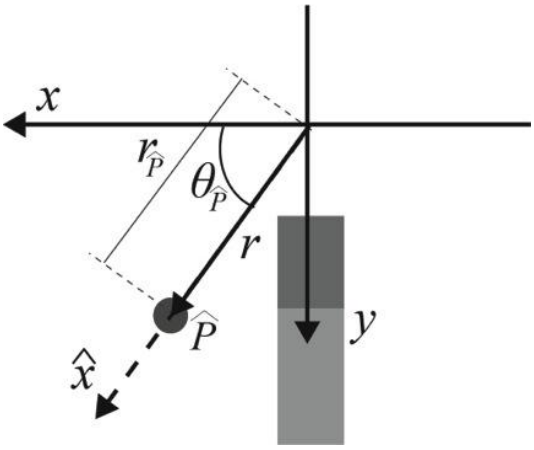

Figure 7. Parameters of the change from Cartesian to cylindrical coordinates

An example of settlement profile S and the correspondent ground horizontal strains $\varepsilon_{h,xx}, \varepsilon_{h,yy}, \varepsilon_{h,xy}$ in the new cylindrical coordinates is shown in Figure 8. The resultant strain $\varepsilon_h \equiv \hat{\varepsilon}_{\hat{x}\hat{x}}$ along the considered alignment ($\theta = 60°$) is given by Eq. (19). The tunnel face location for this particular case is $y_s = 0$m, the tunnel diameter is d=12m, the tunnel depth is z_0=20m, the trough width parameter is K=0.3, the ground volume loss is V_L=1% and the ratio between the settlement at the face and at the tail is δ=0.3.

It can be seen that sagging zone extends from $r = 0$m to $r \approx 17$m and that ε_h is there compressive (negative). Hogging deflection and hence, tensile (positive) values of ε_h, start at $r \approx 17$m. The curves of $\varepsilon_{h,xx}$ and ε_h correspond to the profile of ground strain for $\theta = 0°$ and $\theta = 60°$, respectively. Note the substantial difference between the positive peak values of both curves at $r \approx 22$m. This reduction respect to the transverse case may imply notable variations in the estimation of building damage, as it will be shown later in Sec. 4.

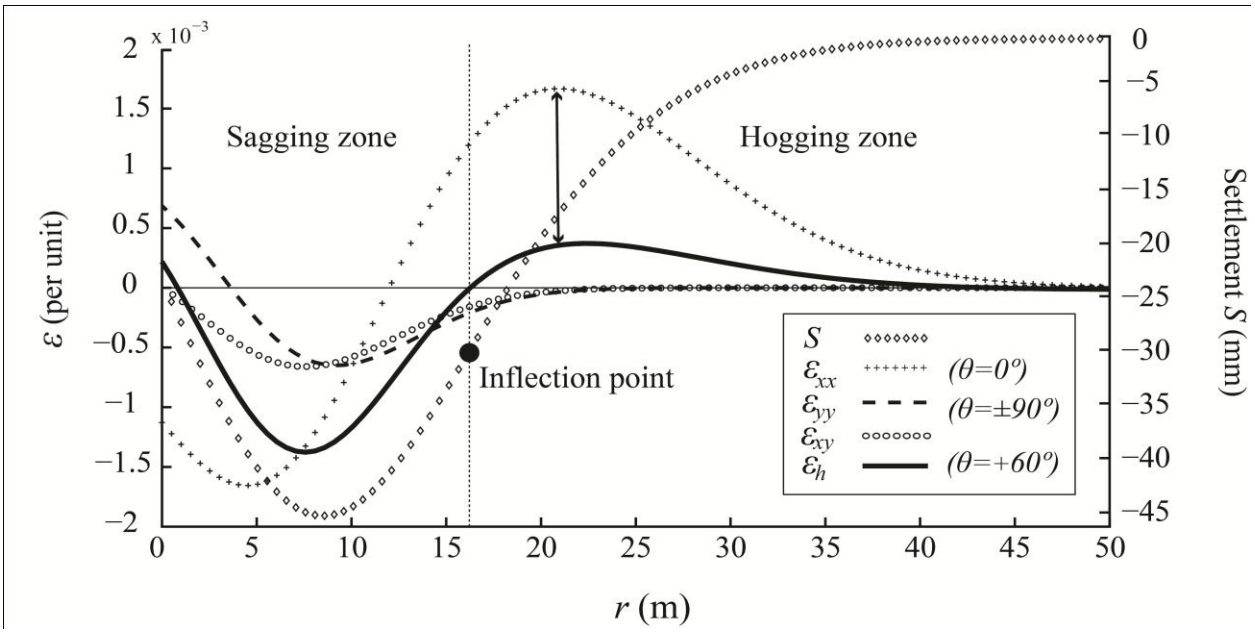

Figure 8. Plot of settlement profile S and ground strains $\varepsilon_{h,xx}$, $\varepsilon_{h,yy}$, $\varepsilon_{h,xy}$ and resultant ε_h at θ=60° for y_s=0m (V_L=1%, K=0.3, δ=0.3, z_0=20m, d=12m).

The variation of ε_h with the alignment θ and the position r for different tunnel face locations is depicted in Figure 9. Note that this Figure represents the extension of Figure 8 for all possible values of θ. It can be seen that the maximum absolute values of ε_{h+} and ε_{h-} are given along $\theta = 90°$ for $r \approx$17m and $r \approx$30m, respectively, when tunnel face is at y_s=+20m (Figure 9a). For $90° > \theta > 45°$, ε_{h+} and ε_{h-} tend to decrease, and for $\theta < 45°$, both ε_{h+} and ε_{h-} become negligible. Therefore, the effect of the excavation when y_s=+20m can only be noticed at alignments close to the longitudinal tunnel axis.

If the tunnel face advances till y_s=0m, the maximum absolute value of compressive strain ε_{h-} is then given at $r \approx$7m for $\theta \approx 50°$ (Figure 9b). The maximum value of ε_{h+} is given at $\theta \approx$ -90°. The intersection of a vertical plane at $\theta =$60° with the plot of ε_h would result in the curve shown in Figure 8. Note also that the less critical θ in terms of ε_{h+} (i.e the range of θ for which ε_{h+} is minimum) is around $\theta \approx$ 60°-70°.

When tunnel face is located at y_s=-20m, both maximum absolute values of ε_{h+} and ε_{h-} occur at $\theta = 0°$ for $r =$ 0m and $r \approx$12m, respectively (Figure 9c). It can be seen that ε_h is 0 for all r if $\theta = +90°$. The reason is that the settlement along this alignment is fully developed and hence, the settlement profile curvature is 0.

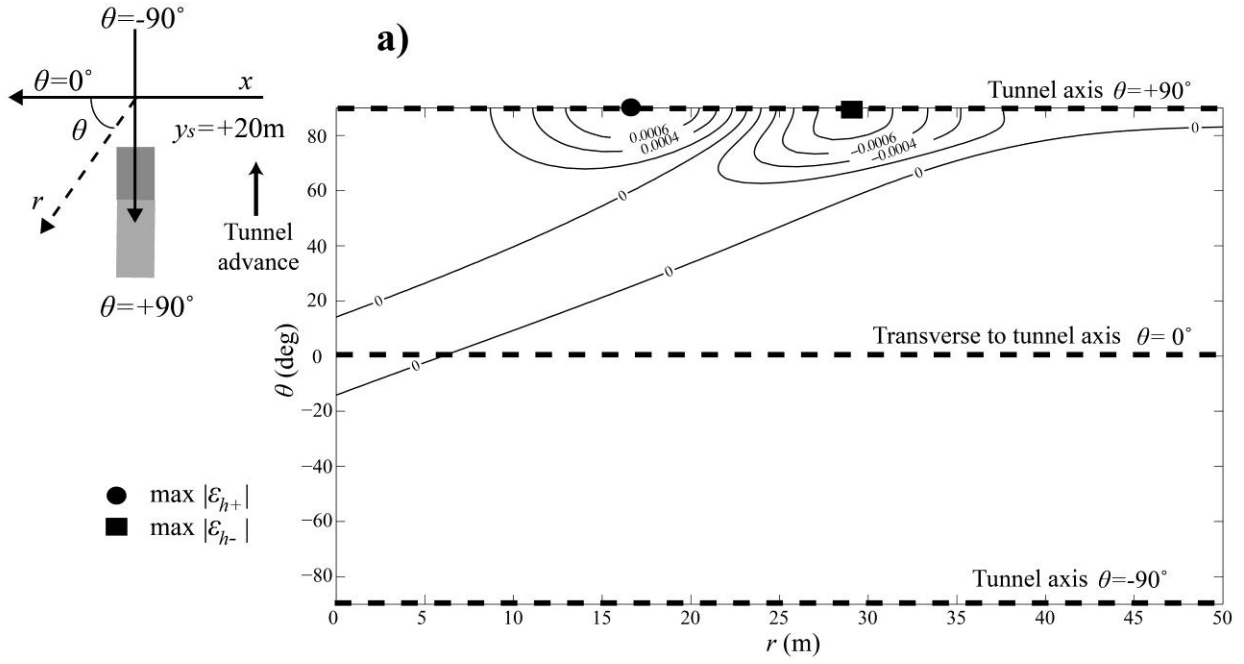
a)
θ=-90°
θ=0°
x
θ
ys=+20m
r
Tunnel advance
θ=+90°
Tunnel axis θ=+90°
Transverse to tunnel axis θ= 0°
Tunnel axis θ=-90°
θ (deg)
r (m)
max |εh+|
max |εh-|

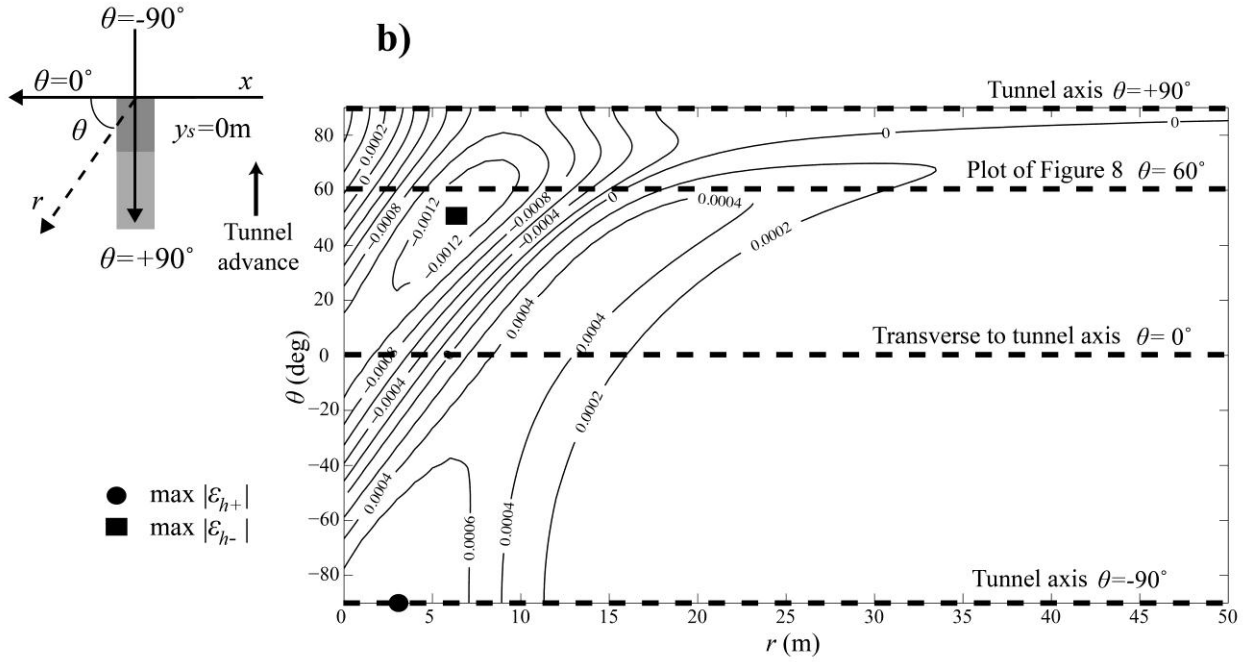
b)
θ=-90°
θ=0°
x
θ
ys=0m
r
Tunnel advance
θ=+90°
Tunnel axis θ=+90°
Plot of Figure 8 θ= 60°
Transverse to tunnel axis θ= 0°
Tunnel axis θ=-90°
θ (deg)
r (m)
max |εh+|
max |εh-|

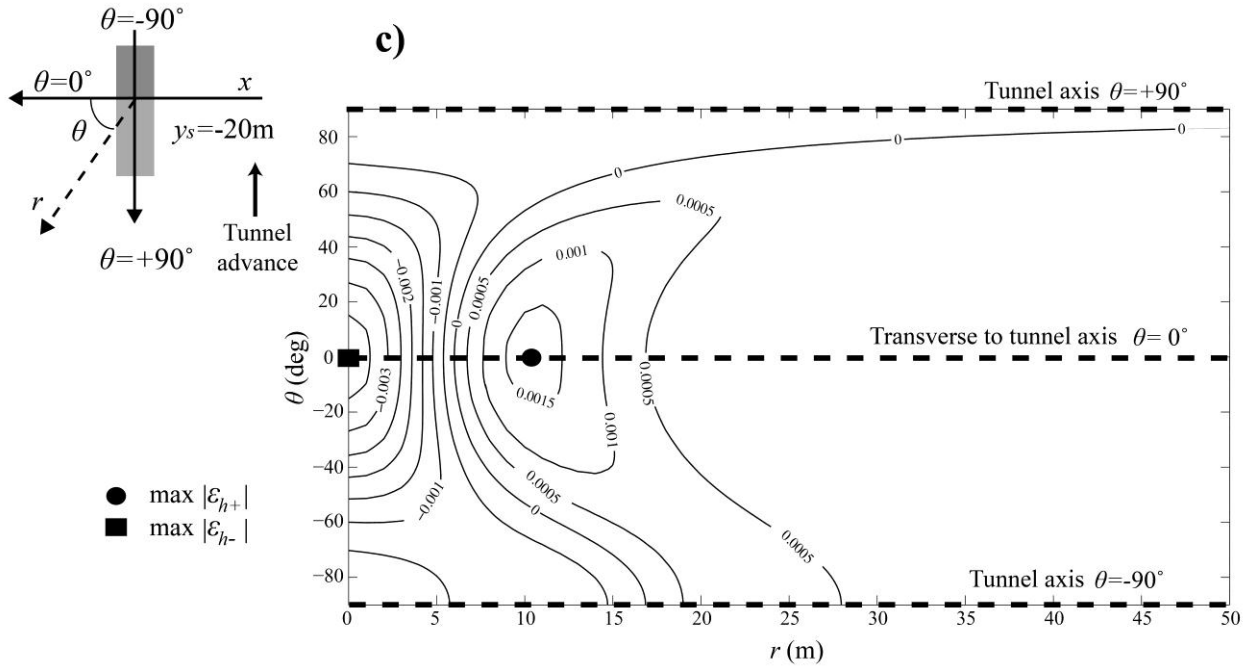

Figure 9. Plot of ε_h for all θ and r if tunnel location is at a) y_s=+20m, b) y_s=0m and c) y_s=-20m (V_L=1%, K=0.3, δ=0.3, z_0=20m, d=12m).

3.3 *Determination of critical values of θ*

The generation of the plots shown in Sec. 3.2 allows identifying possible critical values of θ concerning the maximum absolute values of ε_{h+} and ε_{h-}. For this purpose, the field of ε_h is generated in a parametric analysis for a wide range of ground conditions and tunnel geometries. For every case, the position (r, θ) of the maximum absolute values of ε_{h+} and ε_{h-} is determined by means of optimization techniques. The analysis includes values of K from 0.2 to 0.7 every 0.05; ground volume losses V_L equal to 0.5%, 1%, 1.5% and 2%, which are typical values considered in tunneling engineering; δ ratios equal to 0.5 (as generally assumed) and δ=0.3 for the case of soft soils; tunnel diameters d equal to 8, 10 and 12m and tunnel axis depths z_0 equal to 20, 30 and 40m. The location of the tunnel face y_s spans from +20m to -20m every 10m to simulate the different phases of approximation and underpass of the tunnel face beneath a building wall.

The results show that for tunnel face locations $y_s > 0$ (i.e. tunnel face approaching to the origin of coordinates), the alignment for which ε_{h+} is maximum is $\theta = 90°$, whereas for $y_s < 0$ (i.e tunnel face has underpassed the origin of coordinates), it is $\theta = 0°$. The ratio between the maximum ε_{h+} at $\theta = 0°$ and the maximum ε_{h+} at $\theta = 90°$ is usually between 1.5 and 2. Then, it is clear that the most critical alignment according to the value of ε_{h+} is the transverse direction with respect to the tunnel axis.

Regarding the compressive strains ε_{h-}, the maximum absolute values are given at $\theta = 0°$ when the tunnel face location is $y_s < 0$. However, the trend is not so clear when the tunnel face location is $y_s > 0$. Highest absolute values of ε_{h-} are found in a range of alignments between $\theta = 50°$ and $\theta = 90°$, depending on the geological conditions and the tunnel geometry. The ratio

between the maximum absolute value of ε_{h-} at $\theta = 0°$ and at $\theta \approx 50°$-$90°$ is between 3 and 4. Therefore, the maximum contribution of compressive ground strain ε_{h-} to damage reduction is also at $\theta = 0°$.

3.4 *Discussion*

The presented results show the influence of the alignment θ on the tensile ε_{h+} and compressive ε_{h-} ground horizontal strains. According to the parametric analysis, the maximum absolute values of both ε_{h+} and ε_{h-} are generated for advanced tunnel face locations (i.e. $y_s < 0$) at $\theta = 0°$. Therefore, $\theta = 0°$ is defined as the worst-case scenario regarding ε_{h+}. However, $\theta = 0°$ can give also the maximal contribution of compressive strains ε_{h-} to building damage reduction, but this contribution is generally neglected when using the equivalent beam model, as a conservative practice (see Sec. 4). Hence, $\theta = 0°$ is considered to be the most critical alignment regarding ε_h, independently of the contribution of ε_{h-}. Less critical (lower) values of ε_{h+} may be generated at alignments in between $\theta = 0°$ and 90°. This fact can entail a reduction of the estimated damage when analyses are performed along the real wall alignments θ, instead of doing approximations with the transverse case $\theta = 0°$, as it is usually done in tunneling design.

4. **Relevant aspects of building response modeling in 3D**

4.1 *Introduction*

Sections 2 and 3 showed how to deal with the determination of ground horizontal strain ε_h in a particular wall alignment θ. As seen, this represents a 3D problem governed by the ground properties, the construction technology, the tunnel geometry and the tunnel face position. Once the 2D settlement profile and the correspondent ε_h are determined, the building response is modeled with the equivalent beam method from Burland & Wroth (1974) in order to assess the damages that ground subsidence can produce to the walls. This method is widely used in engineering practice, but however, designers are often not aware of certain aspects that may be critical on the damage predictions.

The present section reviews the application of the equivalent beam method with an advancing tunnel in 3D according to the relative position of the building with respect to the tunnel (Sec. 4.2). The delimitation of the influence area of settlements and its effect on the predictions of building damage is analyzed in Sec. 4.3. The contribution of the ground horizontal strain in sagging zones to damage reduction is analyzed in Sec. 4.4. The influence of the tunnel face location y_s and the building wall alignment θ is studied in Sec. 4.5.

4.2 *Application of the equivalent beam method in 3D*

Maximum tensile strains in the beam for pure bending (ε_{br}) and pure shear (ε_{dr}) modes of deformation (Eqs. (1)-(2)) require the calculation of maximum strains due to the deflection of the beam in pure bending, ε_{bmax}, and pure shear, ε_{dmax}, which are given by the expressions of Burland & Wroth (1974):

$$\varepsilon_{bmax} = \frac{\frac{\Delta}{l}}{\left(\frac{l}{12t} + \frac{3I}{2alH}\frac{E}{G}\right)} \tag{27}$$

$$\varepsilon_{dmax} = \frac{\frac{\Delta}{l}}{\left(1 + \frac{Hl^2}{18I}\frac{G}{E}\right)} \tag{28}$$

where H is the beam height, I is the inertia per unit length which is equal to $H^3/12$, t is the position of the neutral axis and a is the location of the fiber where strains are calculated. In case of sagging deflection, the neutral axis is assumed to be at middle height ($t = H/2$). In case of hogging deflection, the neutral axis is assumed to be at the top fiber ($t = H$) (Figure 10). Strains are calculated in the most critical fiber from the position of the neutral axis, so that $a = t$ in both cases. Δ/l are the maximum deflection ratios for the respective deflection zone: l is the horizontal distance between two reference points and Δ is the relative deflection between these two points. This relative deflection is given by the difference between the settlement profile and the straight lines connecting the settlements at the building extremes and at the inflection points.

The calculation of Eqs. (1)-(2) and (27)-(28) is performed separately for the zones of the building undergoing sagging deflection and for the zones undergoing hogging deflection (Mair et al., 1996). The 3D field of settlements is described by Gaussian curves and therefore, the number of inflection points located along the position of a building can be 0, 1 or 2, depending on its length l_{build}, on the distance from building reference point $\hat{A}$ to the origin of coordinates d_{orig} and on the alignment θ with respect to the tunnel axis. This entails the following cases:

a) The building is subjected only to sagging (short buildings located above the tunnel axis; no inflection points are located along the building).

b) The building is subjected only to hogging (buildings located far from the tunnel longitudinal axis; no inflection points are located along the building).

c) The building is subjected to sagging and hogging (building starts in the zone above the tunnel (sagging) and reaches the hogging deflection zone; 1 inflection point is located along the building).

d) The central part of the building is subjected to sagging and its laterals to hogging (2 inflection points are located along the building).

Therefore, the total length of the building wall l_{build} can be decomposed in three parts: l_{hog_1}, l_{hog_2} and l_{sag} (Figure 10), so that three different deflection ratios can be defined: Δ_{hog_1}/l_{hog_1}, Δ_{hog_2}/l_{hog_2} and Δ_{sag}/l_{sag}. Determination of ε_h in Eqs. (1)-(2) is also performed separately along the length of building zones undergoing sagging and hogging deflection.

The damage on the building wall is then determined depending on the maximum strain ε_{max}:

$$\varepsilon_{max} = \max[\varepsilon_{br}^{sag}, \varepsilon_{dr}^{sag}, \varepsilon_{br}^{hog,1}, \varepsilon_{dr}^{hog,1}, \varepsilon_{br}^{hog,2}, \varepsilon_{dr}^{hog,2}] \tag{29}$$

where ε_{br}^{sag}, $\varepsilon_{br}^{hog,1}$ and $\varepsilon_{br}^{hog,2}$ are the maximum bending strains in sagging and hogging in the three zones, obtained using Eq. (27) and ε_{dr}^{sag}, $\varepsilon_{dr}^{hog,1}$ and $\varepsilon_{dr}^{hog,2}$ are the maximum shear strains in sagging and hogging, obtained using Eq. (28).

ε_{max} is further compared with strain thresholds ε_{lim} that define different categories of damage according to the severity of affection and the typical associated damage, as it can be seen in Table 1.

Table 1. Classification of damage (Burland et al., 1977)

Category of damage	**Normal degree of severity**	**Typical damage**	**Tensile strain ε_{max} (%)**	**ε_{lim}(%)**
0	Negligible	Hair cracks less than 0.1mm	0 – 0.050	0.050
1	Very slight	Fine cracks up to 1mm	0.050 – 0.075	0.075
2	Slight	Cracks easily filled up to 5mm	0.075 – 0.150	0.150
3	Moderate	Cracks from 5 to 15mm	0.150 – 0.300	0.300
4	Severe	Extensive repair works. Cracks from 15 to 25mm	> 0.300	-
5	Very severe	Partial or complete rebuilding. Cracks > 25mm	-	-

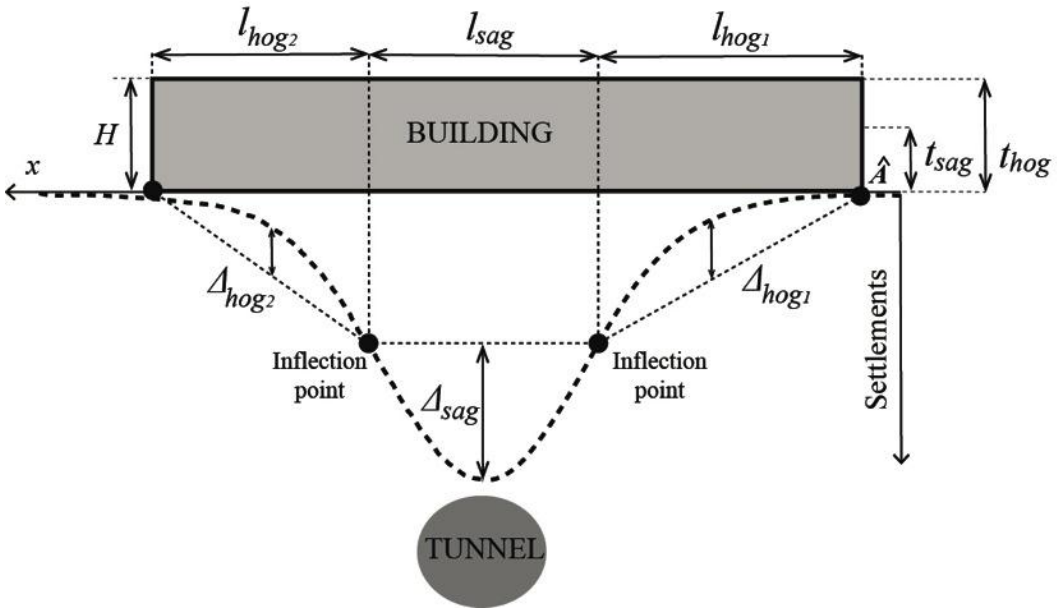

Figure 10. Equivalent beam model – Description of building geometry and deflection ratios

4.3 *Effect of the influence area of settlements on building damage predictions*

4.3.1 *Settlement cut-off*

The influence area of a tunnel construction is defined as the zone where ground subsidence can be generated. Therefore, the infrastructures and buildings inside this area may require a damage assessment prior to the tunnel construction. This area is defined in some tunnel projects as a band of 50m of width at every side of the tunnel axis, but however, other criteria can be used. For example, construction projects in the L9 metro tunnel in Barcelona contained damage assessments only for buildings likely to be affected by settlements higher than 10mm. This limit was reduced to 5mm if the building was of cultural or historical interest.

In Gaussian-shaped settlements troughs, the highest settlements are generated above the tunnel axis and their magnitude decrease exponentially with the distance to tunnel axis. For this reason, buildings can be subjected to high settlements at one side and to negligible at the other. As mentioned in Sec. 4.2, the equivalent beam method needs the calculation of deflections, which depend on the value of settlements at the locations of inflection points and building extremes. Considering the whole length of a building could lead to unreliable estimations of damage due to an overestimation of the deflections Δ, usually in the zones of hogging.

To address this, Mair et al. (1996) proposed to consider the 1mm settlement line to be the limit of the zone of influence. This value was selected in base of the accuracy of monitoring instruments placed along the tunnel track to control ground movements, which is generally around $\pm$1mm. In cases where the building wall overpasses the 1mm area, only the part of the wall subjected to settlements $|S| \geq$1mm is considered. This hypothesis has implications in the calculation of the maximum tensile strain value ε_{max} due to the possible variation of the considered lengths l_{hog_1}, l_{hog_2}, l_{sag}, deflection ratios Δ_{sag}/l_{sag}, Δ_{hog_1}/l_{hog_1}, Δ_{hog_2}/l_{hog_2} (Figure 11) and wall geometry ratios l_{sag}/H, l_{hog_1}/H and l_{hog_2}/H. Moreover, this change of l/H can produce substantial variations on the determination of the most critical mode of deflection, i.e. bending or shear (Burland, 2008). For example, Netzel (2009) show the effect of the influence area in a long structure subjected to subsidence for which the bending strains generated in the beam due to deflection were a 75% higher for the long structure, i.e. considering all the range of settlement, than for the short one, i.e. considering the 1mm settlement line.

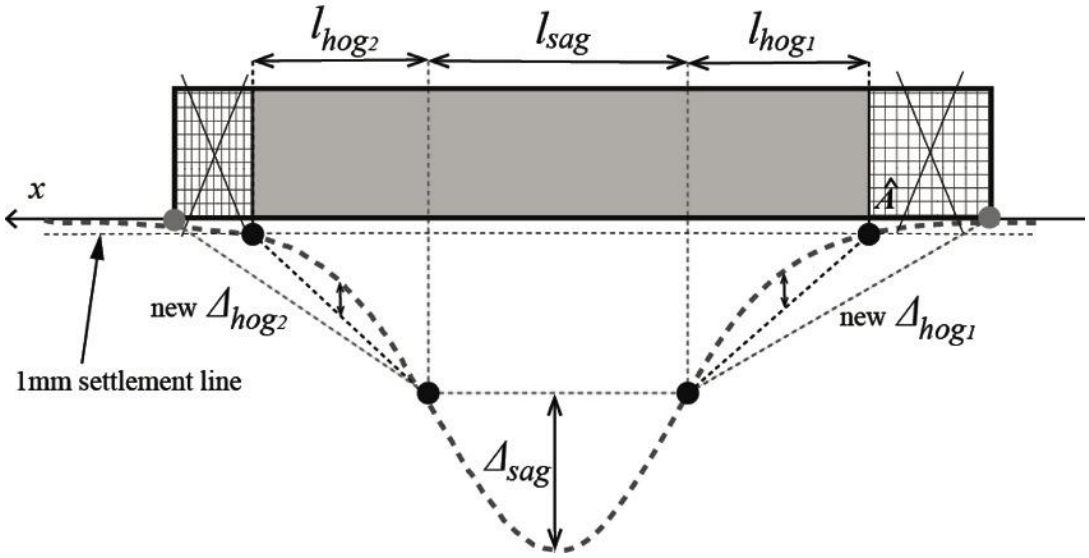

Figure 11. Influence area of settlement troughs and disregarded parts of the building

However, neglecting a part of the building has also implications on the value of ground horizontal strain ε_h. Its magnitude decays with the distance to tunnel axis and therefore, neglecting the zones where settlements are lower than 1mm will give higher ε_{h+} mean values. This will increase the predicted bending ε_{br} and shear ε_{dr} strains (Eqs. (1)-(2)) and hence, the estimated damages in the building will also be higher.

The effect of considering the 1mm settlement line is analyzed now by means of a comprehensive parametric study. For notation convenience, disregarding settlements lower than 1mm will be written as cut-off C_1, whereas including all settlements will be written as cuttoff C_0. A wide

range of geological conditions, tunnel geometries, building position and building geometry is analyzed here (Table 2) to show the differences when considering each criterion. Crossing all the variable values gives a total number of 1,404,480 analyzed cases. The most critical value of ε_{max} along all the tunnel face positions y_s is calculated using both criteria C_0 and C_1.

Table 2. Variable values of the parametric analysis showing the influence of the settlement cut-off

Variable [units]	Description	Analyzed values
K [-]	Trough width parameter	From 0.2 to 0.7, every 0.05
V_L [%]	Ground volume loss	0.05, 1, 1.5, 2
δ [-]	Longitudinal settlement shift ratio	0.3, 0.5
z_0 [m]	Tunnel axis depth	20, 30, 40
d [m]	Tunnel diameter	6, 8, 10, 12
L [m]	Building wall length	10, 20, 30, 40
d_{orig} [m]	Distance from origin of coordinates to wall reference point $\hat{A}$	6, 8, 10, 12
H [m]	Building wall height	3, 6, 9, 12, 15
θ [deg]	Building wall alignment	From 90° to -90°, every 10°
y_s [m]	Tunnel face location	From 60m to -60m, every 5m

The results show a 49% of cases where the estimated ε_{max} is the same using both C_0 or C_1, whereas ε_{max} is lower using C_1 in a 37% of cases and higher in the resting 14%. However, the resulting categories of damage are the same in the 94% of cases, showing that differences of ε_{max} do not generally give significant variations on the damage category estimation. The other 6% of cases give higher or lower categories depending on the values of l_{build}, d_{origin} and l_{build}/H. Table 3 summarizes the differences in the categories and the most relevant parameters of the corresponding buildings. Note that these are the most significant observable parameters of the buildings and do not exclude other possible values to produce the same differences on the damage category estimation.

Table 3. Differences of the estimated category of damage according to the considered settlement cut-off

Difference of estimated category of damage (C_1- C_0)	Percentage of total number of cases	Relevant characteristics of buildings
+4	0.001%	l_{build}/H = 13; d_{orig} =10m; l_{build} =40m
+3	0.032%	l_{build}/H = 10,13; d_{orig} =20m; l_{build} =40m
+2	0.423%	l_{build}/H = 6,10,13; d_{orig} =20m; l_{build} =40m
+1	2.668%	l_{build}/H = 4,6,10 and 13; d_{orig} =15m; l_{build} =30 and 40m
0	94.279%	All types
-1	2.578%	l_{build}/H = from 1 to 3; l_{build} =20, 30 and 40m
-2	0.017%	l_{build}/H = from 1 to 3; l_{build} =20 and 30m

Cases of more than one category of difference represent only the 0.6% of cases. However, the analysis show extreme cases with substantial different estimation of the damage. Cases of +4 categories of difference using C_1 refer to long one-floor buildings starting at tunnel axis. Note also that C_0 could give higher categories in cases of buildings with low l_{build}/H ratios.

The criteria C_1 of Mair et al. (1986) avoids the underestimation of the ground horizontal strain ε_h and thus, it would be more appropriate for the majority of cases. In the remainder of the paper, the analyses will be performed following this criterion.

4.4 *Considering the contribution of ground horizontal strain in sagging zones*

The nature of strain in sagging zones is compressive and therefore, it can contribute to damage reduction. For conservativeness, this contribution is usually neglected and thus the value of ε_{h-} is considered to be equal to 0. This section analyzes which is the effect of considering the mean value of ε_{h-} along the sagging zone.

The values of ε_{max} for the cases of the parametric study shown in Sec. 4.3 are recalculated with this new assumption and further compared. The results show that considering the mean value of ε_{h-} (instead of neglecting it) give the same value of ε_{max} in the 78.6% of cases, a lower value in a 14.3% and a higher value in the resting 7.1%. This increase of ε_{max} is given in some cases where ε_{dr} is higher than ε_{br}. This is so, because considering the mean value of ε_{h-} will always give lower values of ε_{br} (Eq. (1)), but not of ε_{dr} (Eq. (2)). Indeed, low values of ε_{dmax} in sagging (named ε_{dmax}^{sag}) and high mean values of ε_{h-} can lead in higher values of ε_{dr} in sagging (named ε_{dr}^{sag}), with respect to the case of neglecting ε_{h-}. This is shown in Figure 12, where the difference of ε_{dr}^{sag} considering one or the other criteria is depicted. Negative differences of ε_{dr}^{sag} indicate that ε_{dr}^{sag} is higher in the case of neglecting the contribution of ε_{h-} (i.e. the same behavior as in ε_{br}). Contrarily, positive differences indicate that ε_{dr}^{sag} is higher in the case of considering the contribution of ε_{h-}. This can occur for example in long buildings subjected to very sharp profiles for which the generated ground strain ε_{h-} is high and ε_{dmax}^{sag} is low. Note that the plot in Figure 12 does not refer to any particular ground and tunnel parameters, but to a general range of values of ε_{dmax}^{sag} and ε_{h-} introduced in Eq. (2).

The variations of ε_{max} considering one or the other criteria keep however the estimated category of damage in the 97.63% of the total cases. Again, the most significant characteristics of buildings that give differences in the estimated categories of damage are described in Table 4.

Table 4. Difference of estimated category of damage according the value of ε_h in sagging zones

Difference of estimated category of damage (ε_{h-} = mean) - ($\varepsilon_{h-} = 0$)	**Percentage of total number of cases**	**Relevant characteristics of buildings**
+2	0.004%	l_{build}/H = 0.7, 1; d_{orig} =0m, -10m; l_{build} =10m
+1	0.065%	l_{build}/H = 1; d_{orig} =-10m, 0m, 5m; l_{build} =10m
0	97.631%	All types
-1	1.948%	l_{build}/H = 1 to 3; d_{orig} =-10m, 0m, 5m; l_{build} =20m, 30m
-2	0.352%	l_{build}/H = 1 to 3 ; d_{orig} =-10m, 0m, 5m; l_{build} =20m

Note that neglecting the contribution of the ground strain in sagging will be generally conservative, although in some cases it could lead to an underestimation of the damage.

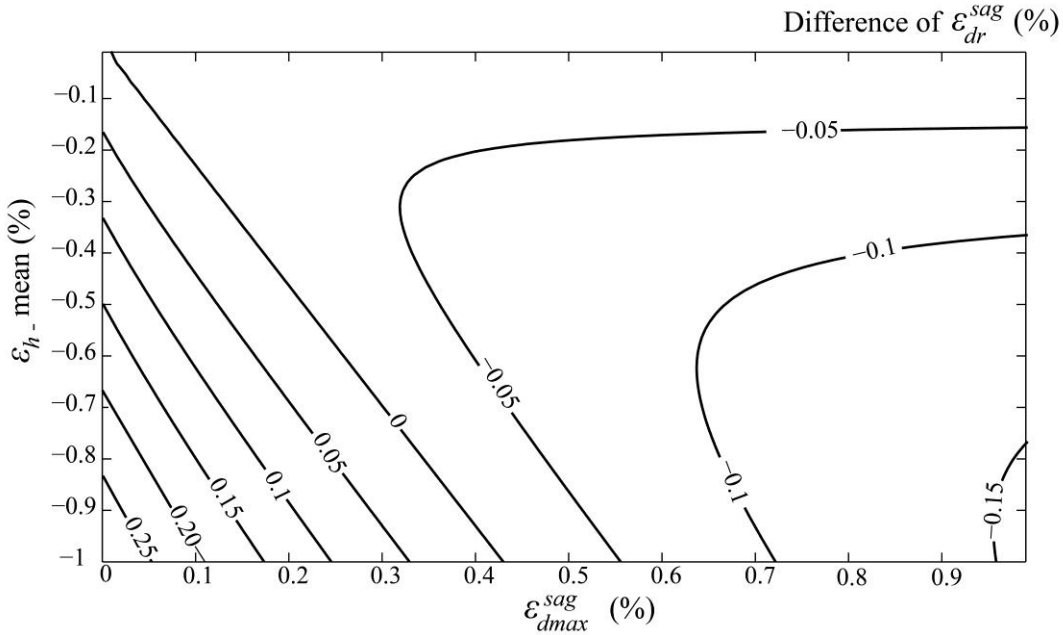

Figure 12. Difference of predicted ε_{dr}^{sag} when the contribution of ε_{h-} is considered or neglected.

4.5 *Influence of the tunnel face location y_s and alignment θ on ε_{max}*

The novel equation proposed in this paper (Eq. (19)) in combination with the Gaussian approximations of the settlement trough and the equivalent beam model allow the determination of ε_{max} in walls located in whichever position with respect to the tunnel axis. The present section analyzes particularly the influence of the alignment θ and the tunnel face location y_s in the assessment of ε_{max}.

Figure 13a) shows an example of the evolution of ε_{max} when the tunnel face advances to $y \rightarrow -\infty$ for different wall alignments θ. The ground parameters and the tunnel geometry are the same as in the example shown in Sec. 3. The building length is L=30m and the height is H=3m. The building corner is located in the origin of coordinates, so that d_{orig} =0m. The material ratio E/G is 2.6, as it is usually assumed for masonry buildings (Burland, 2008).

It can be seen that at θ=+90°, the value of ε_{max} starts to increase for earlier tunnel face locations (approx. at y_s ≈55m). The maximum value of ε_{max} is reached when y_s is in the range of [+25m,+50m] and then it decreases again till zero. This behavior is explained by the fact that after the tunnel underpass, the longitudinal settlement is fully developed and hence the curvature is zero, so that both Δ and ε_h become zero. Obviously, the plot of ε_{max} for θ=-90° at Figure 13b) is identical with a shift in the y^- direction.

For θ=+60°, +30° and 0°, the maximum value of ε_{max} is given after the tunnel face underpass beneath the building. However, note that ε_{max} and the associated categories of damage will be substantially different for the three alignments: category 2 for θ=+60°, category 3 for θ=+30° and category 4 for θ=0°. For θ=-60° and θ=-30°, ε_{max} tends to the same values as for the corresponding positive alignments. However, the peak values that are achieved during the tunnel

face underpass are different, which make pictures non identical. This variation is more significant in the case of θ=-60°: the peak value of ε_{max} is given at earlier y_s than for θ=+60°.

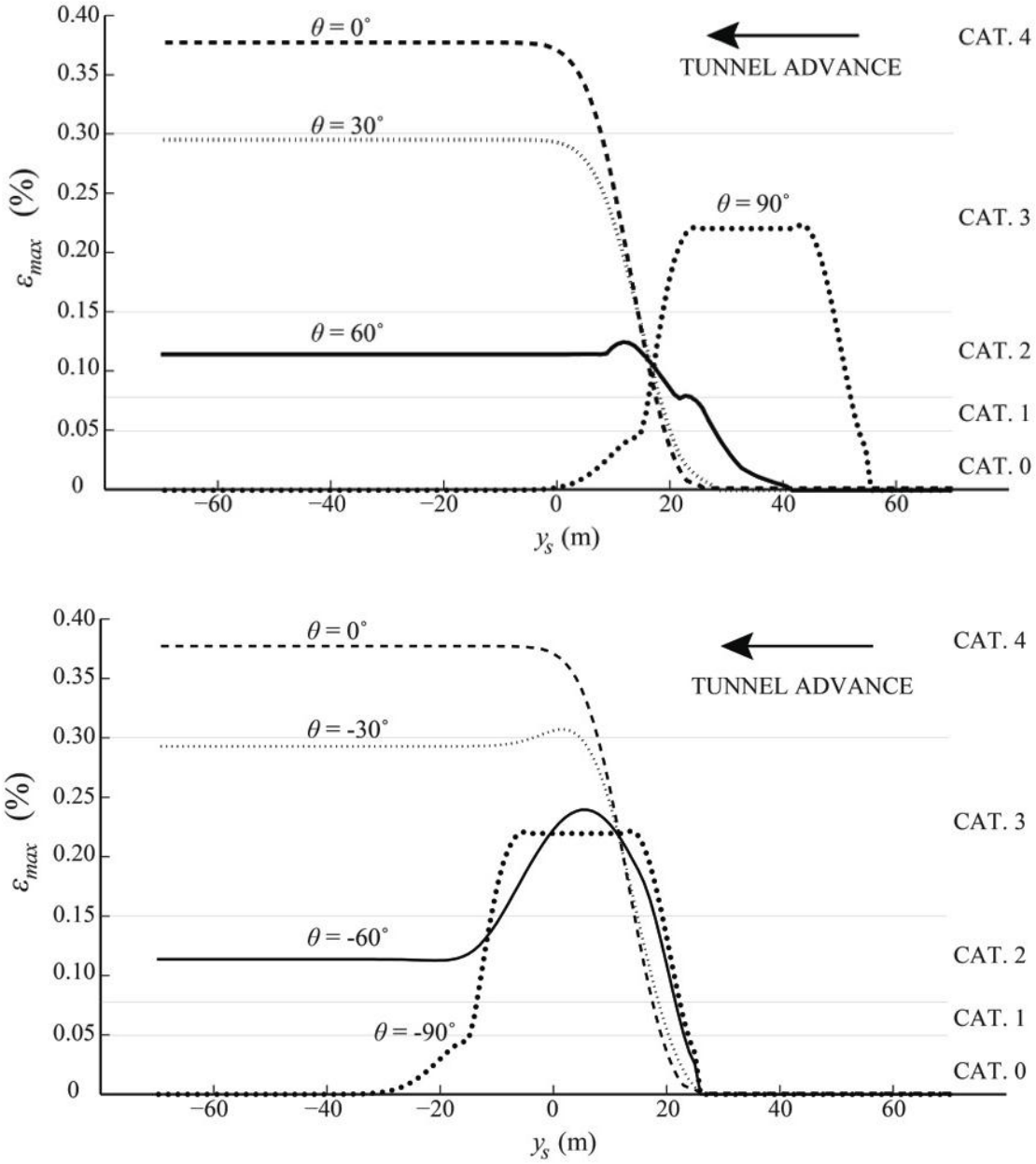

Figure 13. Evolution of ε_{max} for an advancing tunnel face from y_s =70m to y_s = −70m for a) θ =+90°, +60°, +30°, 0° and b) θ =-90°, -60°, -30°, 0° (L =30m, d_{orig} =0m, H =3m, E/G =2.6, z_0 =20m, d =12m, K =0.3, V_L =1%, δ =0.3).

It is also of interest to observe the variation of ε_{max} with θ for fixed tunnel face locations y_s. For this purpose, the plot of ε_{max} for a range of θ between [+90°,-90°] and y_s=+30, +10, 0 and -30m is depicted in dashed lines in Figure 14. It can be seen that the most critical alignment is θ =90° when tunnel face is approaching to the building (y_s=+30) and θ =0° for the rest of y_s.

The envelope of the maximum value of ε_{max} for each position of tunnel face y_s is depicted in the same figure with a solid line. As it could be expected, the peak value of ε_{max} is given at θ =0°. This agrees with the alignment for which the tensile ground horizontal strain ε_{h+} was maximal (shown in Sec. 3). Moreover, it is evident that the maximum deflections Δ will also be given along θ =0°. The interesting point here is to see the notably reduction of damage that can be given for θ ≠0°. Minimum damages are achieved for wall alignments close to θ ≈+65°, which matches with the direction of minimum ε_{h+} that was shown in Sec. 3.2. The reduction of ε_{max} in this case is about the 70%, which implies a difference of 2 categories of damage with respect to the transverse case.

Note that all the presented results refer to a particular example that was chosen for illustrations purposes. The value of θ plays here a key role in the assessment of damage but however, the influence of θ may not be so critical for other combination of ground parameters, building locations and tunnel and building geometries. It is also important to note that the present novel formulation does not conflict with the typical analyses that assume the building located transverse to the tunnel axis. As it has been shown, this represents the worst-case scenario but however, significant reductions of estimated damage may be achieved if the real wall alignment θ is considered, thus avoiding possible overestimation of predicted damages.

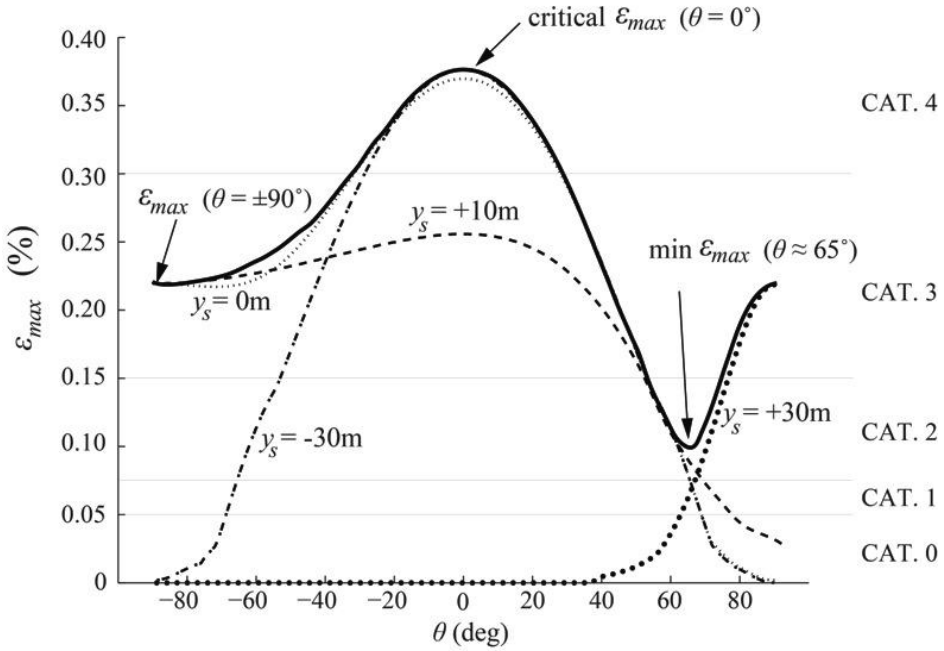

Figure 14. Envelope of ε_{max} for an advancing tunnel face from θ =90° to -90° for y_s =+30m, +10m, 0m and -30m (L =30m, d_{orig} =0m, H =3m, E/G =2.6, z_0 =20m, d =12m, K =0.3, V_L =1%, δ =0.3).

The consideration of the wall alignment θ has practical implications in tunneling design, for example in the choice of the tunnel depth. For this particular example, if the damage assessment is done for θ =0°, the minimum tunnel depth z_0 for which ε_{max} does not cross the threshold of category 0 of damage (ε_{lim} =0.050%) is 50m. On the contrary, if the wall alignment is for example θ =60°, the minimum depth that fulfills damage requirements is 30m (consider that neither the diameter d nor the expected volume loss V_L can be decreased). The difference of 20m of depth may have important economical implications, since construction costs of tunnels increase with the depth. Obviously, other less drastic measures could be implemented to avoid

this large increase of depth, such as the construction of retaining walls or the stabilization of ground with grout injection. Nevertheless, their effect cannot be taken into account with the presented methodology.

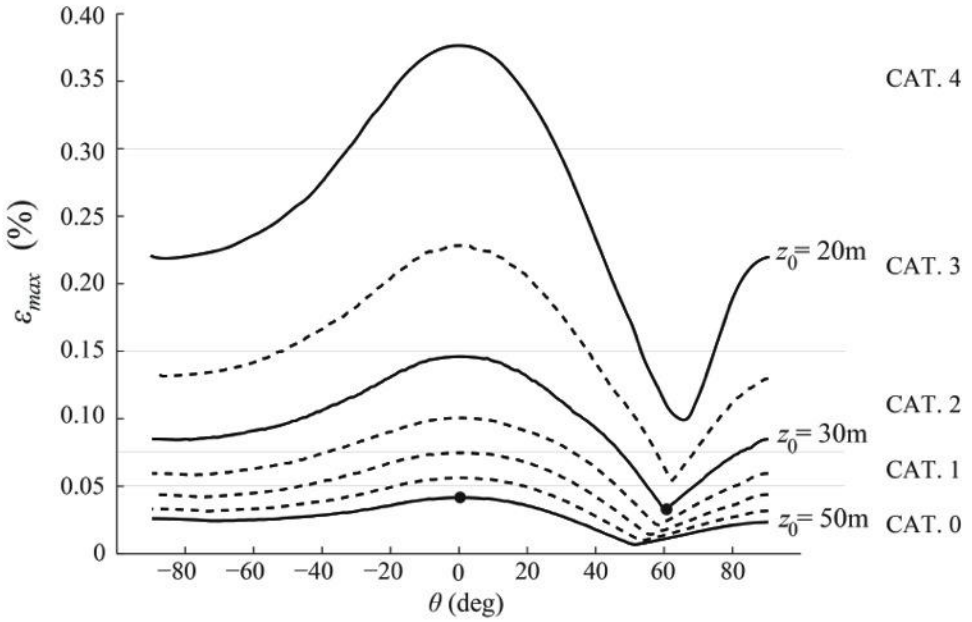

Figure 15. Evolution of ε_{max} for an advancing tunnel face from θ =90° to -90° at different z_0 for the most critical tunnel face location y_s (L =30m, d_{orig} =0m, H =3m, E/G =2.6, d =12m, K =0.3, V_L =1%, δ =0.3).

All the proposed models in Sections 2, 3 and 4 can be used in combination with reliability techniques to take into account the uncertainty regarding the settlement trough models and the building response, as shown in Camós, Špačková et al. (2014).

5. Non-linear parametric regression model for direct estimation of ε_{max}

The process of determining ε_{max} comprises several steps including (1) the determination of the settlement trough according to tunnel geometry and ground conditions, (2) the determination of the influence area where $|S| \geq$1mm, (3) the delimitation of zones subjected to sagging and hogging deflection, (4) the determination of the profile of ε_h and (5) the calculation of deflection ratios Δ/L. No expression has been found in the literature to directly estimate the value of ε_{max} for given input parameters V_L, K, z_0, d, L, H and d_{orig}. For this reason, the results generated in the parametric analysis of Sec. 4 are used to adjust a non-linear parametric regression model (named $\varepsilon_{max,fit}$) that fits the output values of ε_{max} for every combination of ground, tunnel and building wall. The proposed model has been inspired in the equations for describing the Gaussian settlement profile in the transverse direction with respect to the tunnel axis and applies only for the case $\theta = 0°$. Therefore, only the value of ε_{max} at $y_s = -\infty$ (i.e. the most critical) is considered:

$$\varepsilon_{max,fit} = A \cdot exp(B) \tag{30}$$

where,

$$A = \frac{V_L \cdot d^2}{K^2 \cdot z_0^2} \cdot H^{\alpha_1} \tag{31}$$

And,

$$B = \alpha_2 + \alpha_3 \frac{L}{H} + \alpha_4 d_{orig} + \alpha_5 \left(\frac{L}{H}\right)^2 + \alpha_6 d_{orig} \frac{L}{H} + \alpha_7 d_{orig}^2 + \alpha_8 L^2 d_{orig} + \alpha_9 d_{orig} L$$
$$+\alpha_{10} d_{orig}^2 L + \alpha_{11} K z_0 + \alpha_{12} (K z_0)^2 + \alpha_{13} K z_0 d_{orig} + \alpha_{14} H \tag{32}$$

where L, H, z_0, d and d_{orig} are given in [m], V_L is introduced per unit value and K is non-dimensional. The output value of $\varepsilon_{max,fit}$ is directly given in [%]. The regression coefficients α_i obtained by least squares estimation (Smyth, 2006) are summarized in Table 5 for cases of $d_{orig} \geq 0$ and $d_{orig} < 0$. The purpose of this separation is the improvement the adjustment. The range of variable values for which the model is applicable is: V_L from 0.5% to 2%, K from 0.25 to 0.7, z_0 from 20m to 40m, d from 8m to 12m, L from 10m to 40m, H from 3m to 15m and d_{orig} from -40m to 20m.

Table 5. Regression coefficients for the determination of ε_{max} with Eq. (30)-(32) ($\theta = 0°$).

	α_1	α_2	α_3	α_4	α_5	α_6	α_7
$d_{orig} \geq 0$	0.75188	-0.65019	0.24838	-0.049307	-0.011983	-0.0011347	-0.0065007
$d_{orig} < 0$	0.95388	-0.17492	0.20823	-0.020049	-0.0078135	0.00094454	-0.0031526
	α_8	α_9	α_{10}	α_{11}	α_{12}	α_{13}	α_{14}
$d_{orig} \geq 0$	$-3.0141 \cdot 10^{-6}$	-0.0013133	$4.0938 \cdot 10^{-5}$	0.27747	-0.017491	0.016701	-0.052683
$d_{orig} < 0$	$6.1548 \cdot 10^{-5}$	-0.002026	$6.7886 \cdot 10^{-5}$	0.061016	-0.0073386	-0.0037471	-0.0796

The case of $d_{orig} \geq 0$ has been adjusted with 28800 observations and shows a coefficient of determination R^2=0.91. The case of $d_{orig} < 0$ is adjusted with 38400 observations with R^2=0.92. The predicted values of $\varepsilon_{max,fit}$ match in category of damage in the 81% of cases with the categories given by the exact results of ε_{max}. Differences of 1 category of damage are given in the 16% of cases and differences of 2 categories or more in about the 3%.

In general terms, the proposed equation represents well the variation of ε_{max} with the input parameters in the majority of cases. However, the value of $\varepsilon_{max,fit}$ may be overestimated if ε_{max} is expected to be very low. This can occur for example with walls positioned far from the tunnel axis (i.e. with high positive values of d_{orig}). For this reason, the use of this expression should be limited to cases of preliminary assessments of damage.

6. **Conclusion**

The paper proposes a novel equation for the determination of the ground horizontal strain along an alignment θ with respect to the tunnel axis. This equation comes from the application of the strain tensor theory to the classical Gaussian models that describe the settlement troughs generated by tunnel construction. The proposed methodology allows the modeling of the effect

of the tunnel face advance on the settlement profiles, as well as applying the equivalent beam method for whichever position of the building walls in 3D.

Building damage predictions usually assume that walls are located transverse to the tunnel axis (θ =0°). This represents the worst-case scenario and a conservative practice. The reason is because ground horizontal strain and deflections are maximal along this alignment. The novel formulation allows considering the real building wall alignment θ and hence, the possibility of reducing the estimated damage on buildings, which can be significant for some cases. An example was shown where the reduction of ε_{max} was about the 70%.

The presented formulation allows also determining the position of the tunnel face y_s along the tunnel track for which damages in walls are maximal. In cases of θ =0°, the most critical position y_s is always at $y_s \to -\infty$, i.e. after the tunnel face underpass beneath the building. However, in cases where $\theta \neq$0°, the value of y_s that maximizes ε_{max} can be given during the tunnel approach and hence, an iterative analysis should be performed to determine it. A general procedure is developed to calculate the most critical tunnel face location. For example, in case of longitudinal buildings with respect to the tunnel axis, the most critical situation tends to be when the tunnel face reaches the building corner.

Furthermore, a comprehensive parametric analysis has been performed for a wide range of geological conditions, walls and tunnel geometries in order to review relevant aspects of building damage predictions in 3D. The importance of delimiting the influence area of settlements has been shown. Overestimation of deflections Δ and underestimation of tensile ground strain ε_{h+} may occur in case of long buildings subjected to a high variation of differential settlements along its length. To avoid this, the part of the buildings subjected to settlements lower than 1mm should be disregarded.

The data generated in the parametric analysis is used to create a non-linear regression model for making preliminary damage assessments. The model allows direct estimation of the maximum tensile strain ε_{max} in building walls aligned θ =0° for given input values of geological conditions and wall and tunnel geometries. The presented model shows a good fit of the data and foresees the category of damage correctly in more than 80% of the cases.

Acknowledgements

The Spanish Ministry of Economy and Competitiveness (MINECO) and the ERDF (European Regional Development Funds) have funded this research in the framework of the SUBTIS project ('Study of the Sensitivity of Urban Tunnels to Tunneling Induced Settlements' – BIA-2009-13233) by means of a pre-doctoral scholarship (FPI – BES-2010-030132).

REFERENCES

Abramowitz, M. and Stegun, I. A. (1972). Handbook of Mathematical Functions with Formulas, Graphs and Mathematical Tables, 9th printing. New York: Dover, p.11.

Attewell, P. B. and Woodman, J. P. (1982) *Predicting the dynamics of ground settlement and its derivatives caused by tunnelling in soil*. Ground Engineering, 15 (7), 13-22 & 36.

Attewell, P.B., Yeates, J. and Selby, A.R. (1986) Soil movements induced by tunneling and their effects on pipelines and structures. Blackie Academic & Professional, Glasgow

Boscardin, M.D. and Cording, E.J. (1989) *Building response to excavation-induced settlement.* Journal of Geotechnical Engineering, ASCE , 115(1), 1-21

Burland. J.B. (2008) The assessment of the risk of damage to buildings due to tunnelling and excavations. Jornada Técnica Payma Cotas: Movimiento de edificios inducidos por excavaciones. pp. 3.

Burland, J.B., Broms, B. and De Mello,V.F.B. (1977) *Behaviour of foundations and structures*. Proc. 9th International Conference on Soil Mechanics and Foundations Eng., 2, 495-546.

Burland, J.B. and Wroth, C.P., (1974). Settlement of buildings and associated damage. London: Pentech Press.

Camós, C., Molins, C. and Arnau, O. (2014). *A case study of damage on masonry buildings produced by tunneling induced settlements*. International Journal of Architectural Heritage, 8, 602-625.

Camós, C., Špačková, O., Straub, D. and Molins, C. (2014) *Probabilistic approach to assessing and monitoring settlements caused by tunneling*. Submitted to the Tunnelling and Underground Space Technology journal.

Fargnoli, V., Boldini, D., Amorosi, A. (2013). *TBM tunnelling-induced settlements in coarse-grained soils: The case of the new Milan underground line 5*. Tunnelling and Underground Space Technology 38: 336–347

Giardina G., Van de Graaf, A.V., Hendriks, M.A.N, Rots, J.G. and Marini A. (2013). *Numerical analysis of a masonry facade subject to tunnelling-induced settlements*. Engineering Structures 54 (2013): 234–247

Giardina G., Marini A., Hendriks, M.A.N, Rots, J.G. and Rizzardini, F., Giuriani, E. (2012). *Experimental analysis of a masonry facade subject to tunnelling-induced settlements*. Engineering Structures 45 (2012): 421–434

Smyth, G.K. (2006). *Nonlinear regression*. Encyclopedia of Environmetrics 3: 1405–1411. John Wiley & Sons, Ltd. Chichester, UK.

Kappen, J.M.J. (2012). Three-dimensional numerical analysis of tunnelling induced damage: the influence of masonry building geometry and location. Master Thesis, Delft University of Technology (The Netherlands).

Netzel, H. (2009). Building response due to ground movements. Doctoral Thesis, Delft University of Technology (The Netherlands).

Nomoto, T., Mori, H., Matsumoto, M., 1995. *Overview on ground movements during shield tunnelling – a survey on Japanese shield tunnelling*. In: Proc. Int. Symposium on Geotechnical Aspects of Underground Construction in Soft Ground, Balkema, pp. 345–35

O'Reilly, M. P. and New, M. 1982. *Settlements above tunnels in the United Kingdom—Their magnitude and prediction*. In Proceedings of Tunnelling '82. London, UK: Institution of Mining and Metallurgy, 173–181.

Peck, R.B. (1969) *Deep excavations and tunneling in soft ground*. SOA Report, 7th Int. Conf. SM&FE.

ANNEX

A. Development of Eq. (21)

Application of Eq. (19) requires the calculation of the term $\frac{\partial U_x}{\partial y}$, given in Eq. (21). It has been assumed that:

$$\frac{\partial U_x}{\partial y} = \frac{\partial\left(\frac{x}{z_0 - z}\cdot S\right)}{\partial y} = \frac{\partial\left(\frac{x}{z_0 - z}\cdot S\right)}{\partial y} = \frac{x}{z_0 - z}\cdot\frac{\partial S}{\partial y} \tag{A.1}$$

where:

$$\frac{\partial S}{\partial y} = -S_{max}\cdot exp\left[-\frac{x^2}{2\cdot K_x^2\cdot(z_0 - z)^2}\right]\cdot \tag{A.2}$$
$$\cdot\frac{\partial}{\partial y}\left(\left[\Phi\left(\frac{y-(y_s+y_0)}{K_y\cdot(z_0-z)}\right)-\Phi\left(\frac{y-y_f}{K_y\cdot(z_0-z)}\right)\right]\right)$$

Focusing on the derivatives:

$$\frac{\partial}{\partial y}\left(\left[\Phi\left(\frac{y-(y_s+y_0)}{K_y\cdot(z_0-z)}\right)-\Phi\left(\frac{y-y_f}{K_y\cdot(z_0-z)}\right)\right]\right) \tag{A.3}$$
$$= \frac{\partial\left[\Phi\left(\frac{y-(y_s+y_0)}{K_y\cdot(z_0-z)}\right)\right]}{\partial y} - \frac{\partial\left[\Phi\left(\frac{y-y_f}{K_y\cdot(z_0-z)}\right)\right]}{\partial y}$$

Renaming these two derivatives as *C* and *D*:

$$C = \frac{\partial\left[\Phi\left(\frac{y-(y_s+y_0)}{K_y\cdot(z_0-z)}\right)\right]}{\partial y} \tag{A.4}$$

$$D = \frac{\partial\left[\Phi\left(\frac{y-y_f}{K_y\cdot(z_0-z)}\right)\right]}{\partial y} \tag{A.5}$$

Φ corresponds to the standard normal cumulative distribution function:

$$\Phi = \int_{-\infty}^{f(y)}\frac{1}{\sqrt{2\pi}}e^{-\frac{m^2}{2}}dm \tag{A.6}$$

where m is an auxiliary integration variable.

The field of ground displacements (and hence, the strain tensor $\boldsymbol{\varepsilon}$) at a particular depth z is given for each combination of ground conditions and tunnel geometry values (K_x, K_y, y_0, z_0, V_L, D, y_s and y_f). Therefore, the derivatives *C* and *D* in Eq. (A.3) will depend only on the variable y. The functions $f_C(y)$ and $f_D(y)$ at C and D are:

$$f_C(y) = \frac{y - (y_s + y_0)}{K_y \cdot (z_0 - z)} \tag{A.7}$$

$$f_D(y) = \frac{y - y_f}{K_y \cdot (z_0 - z)} \tag{A.8}$$

In this case, the Leibniz integral rule applies (Abramowitz et al., 1972):

$$\frac{d}{dy}\left(\int_{f_1(y)}^{f_2(y)} g(m)dm\right) = g[f_2(y)] \cdot f_2'(y) - g[f_1(y)] \cdot f_1'(y) \tag{A.9}$$

where f_1, f_2 are g are generic functions that depend on y and f_1' and f_2' are the correspondent derivatives respect to y. Since the lower bound of both integrals in C and D is $-\infty$, $f_1' = 0$ and Eq. (A.9) results in:

$$\frac{d}{dy}\left(\int_{-\infty}^{f_2(y)} g(m)dm\right) = g[f_2(y)] \cdot f_2'(y) \tag{A.10}$$

So that, if $f_2 \equiv f_C(y)$,

$$C = \frac{d\left[\Phi\left(\frac{y-(y_s+y_0)}{K_y \cdot (z_0-z)}\right)\right]}{dy} = \frac{1}{\sqrt{2\pi}} e^{-\frac{\left(\frac{y-(y_s+y_0)}{K_y \cdot (z_0-z)}\right)^2}{2}} \cdot \left(\frac{1}{K_y \cdot (z_0 - z)}\right) \tag{A.11}$$

And if $f_2 \equiv f_D(y)$,

$$D = \frac{d\left[\Phi\left(\frac{y-y_f}{K_y \cdot (z_0-z)}\right)\right]}{dy} = \frac{1}{\sqrt{2\pi}} e^{-\frac{\left(\frac{y-y_f}{K_y \cdot (z_0-z)}\right)^2}{2}} \cdot \left(\frac{1}{K_y \cdot (z_0 - z)}\right) \tag{A.12}$$

Then, the component of the strain tensor is finally obtained:

$$\frac{\partial U_x}{\partial y} = \frac{x}{z_0 - z} \cdot (-S_{max}) \cdot \left(exp\left(-\frac{x^2}{2 \cdot K_x^2 \cdot (z_0 - z)^2}\right)\right) \cdot (C - D) \tag{A.13}$$

which is equivalent to Eq. (21).

B. Notation

a	Height of the equivalent beam fiber where strains are calculated
C_0	Cutt-off 0 (settlements lower than 1mm are included)
C_1	Cutt-off 1 (settlements lower than 1mm are disregarded)
d	Tunnel diameter

d_{axis}	Distance from tunnel longitudinal axis to a parallel building wall
d_{orig}	Distance from origin of coordinates to building
E/G	Material elastic / shear modulus ratio
H	Building height
I	Inertia per unit length of the equivalent beam
i_x (or i)	Distance from origin to inflection point in the transverse direction to tunnel axis
i_y	Distance from origin to inflection point in the longitudinal direction to tunnel axis
K_x (or K)	Settlement profile shape parameter in the transverse direction to tunnel axis
K_y	Settlement profile shape parameter in the longitudinal direction to tunnel axis
l_{hog_1}	Building length in hogging zone 1
l_{hog_2}	Building length in hogging zone 2
l_{build}	Building length
l	Horizontal distance between two reference points
l_{sag}	Building length in sagging zone
r	Horizontal distance between the z-axis and whichever point
$r_{\hat{P}}$	Horizontal distance between the z-axis and whichever ground point $\hat{P}$
S	Settlement
S_{max}	Maximal settlement
S_{par}	Settlement for buildings walls parallel to tunnel axis
t	Position of neutral axis in the equivalent beam
t_{hog}	Position of neutral axis in the hogging zone of the equivalent beam
t_{sag}	Position of neutral axis in the sagging zone of the equivalent beam
U_x	Ground horizontal movements in the transverse direction (to tunnel axis)
U_y	Ground horizontal movements in the longitudinal direction (to tunnel axis)
$U_{y,par}$	Ground horizontal movements for buildings walls parallel to tunnel axis
V_L	Ground volume loss
x	x-coordinate
$\hat{x}$	$\hat{x}$-coordinate
y	y-coordinate
y_0	Horizontal shift of longitudinal settlement profile
y_f	Distance from origin of coordinates to tunnel end
y_s	Distance from origin of coordinates to tunnel face
z	z-coordinate
z_0	Depth of tunnel axis
$z_{\hat{P}}$	Depth of whichever ground point $\hat{P}$
Δ	Relative deflection between two reference points
Δ/l	Deflection ratio
Δ_{sag}/l_{sag}	Deflection ratio in sagging zone
Δ_{hog_1}/l_{hog_1}	Deflection ratio in hogging zone 1
Δ_{hog_2}/l_{hog_2}	Deflection ratio in hogging zone 2
δ	Ratio between surface settlement above tunnel face and maximal settlement at infinite distance of the face
ε_{bmax}	Maximum tensile strain in the equivalent beam due to bending
$\varepsilon_{br}^{hog,1}$	Maximum bending strain in hogging zone 1

$\varepsilon_{br}^{hog,2}$	Maximum bending strain in hogging zone 2
ε_{br}^{sag}	Maximum bending strain in sagging zone
ε_{br}	Resultant extreme fiber strain in bending, accounting for ground strain
ε_{dmax}	Maximum tensile strain in the equivalent beam due to shear
ε_{dmax}^{sag}	Maximum tensile strain in the equivalent beam due to shear in sagging zone
$\varepsilon_{dr}^{hog,1}$	Maximum shear strain in hogging zone 1
$\varepsilon_{dr}^{hog,2}$	Maximum shear strain in hogging zone 2
ε_{dr}^{sag}	Maximum shear strain in sagging zone
ε_{dr}	Resultant extreme fiber strain in shear, accounting for ground strain
ε_{h}^{sag}	Resultant horizontal ground strain at surface in sagging zone
ε_{h}	Resultant horizontal ground strain
ε_{h+}	Tensile horizontal ground strain
ε_{h-}	Compressive horizontal ground strain
$\varepsilon_{h,par}$	Resultant horizontal ground strain for buildings walls parallel to tunnel axis
ε_{lim}	Limit strain value for damage classification
ε_{max}	Maximum strain in the equivalent beam
$\varepsilon_{max,fit}$	Adjusted maximum strain in the equivalent beam (non-linear regression model)
$\varepsilon_{h,xx}$	Component xx of ground strain infinitesimal tensor
$\hat{\varepsilon}_{h,\widehat{xx}}$	Component $\widehat{xx}$ of ground strain infinitesimal tensor
$\hat{\varepsilon}_{h,\widehat{xx},par}$	Component $\widehat{xx}$ of ground strain infinitesimal tensor for buildings walls parallel to tunnel axis
$\varepsilon_{h,xy}$	Component xy of ground strain infinitesimal tensor
$\varepsilon_{h,yy}$	Component yy of ground strain infinitesimal tensor
θ	Building alignment respect to x axis
$\theta_{\hat{P}}$	Alignment of whichever ground point $\hat{P}$
$\Phi(\cdot)$	Cumulative standard normal distribution function